A Comparative Analysis of Expression Patterns of *occ1* mRNA in Mammalian Brains

By Toru Takahata

Department of Basic Biology, School of Life Science, The Graduate University for Advanced Studies

Division of Brain Biology, National Institute for Basic Biology

June 2005

Contents

Summary

occl is a gene whose expression is particularly abundant in neurons in the macaque primary visual cortex (V1). In the present study, I report that the expression of *occl* mRNA in the macaque neocortex can be classified into two modes. The first mode is associated with excitatory neurons distributed in the major thalamocortical recipient layers that exhibit strong cytochrome oxidase activity. This is highly prominent in V1. The second mode is associated with parvalbumin-positive GABAergic interneurons and is distributed across the macaque neocortex. In V1, monocular deprivation showed that *occl* mRNA expression in excitatory neurons was markedly dependent on afferent activity, whereas that in GABAergic interneurons was not. Cross-species comparison showed specific differences in cortical expression, whereas subcortical expression pattern was similar between species. In marmosets, a strong expression was observed in V1 similarly to macaques; but the expression of *occl* mRNA was weak in the mouse neocortex. In rabbit and ferret cortices, the strong expression was observed only in GABAergic interneurons. Finally, strong *occl* mRNA expression was observed in many excitatory, glutamatergic sensory relay nuclei in the mouse subcortex, but was not activity-dependent. I conclude that activity-dependent *occl* mRNA expression in the excitatory neurons of V1 was caused by a novel mechanism acquired by primates after their separation from other lineages.

Introduction

The mammalian neocortex is subdivided into functionally and anatomically distinct areas (Brodmann, 1909). There have been long-standing debates as to what extent the specification of neocortical areas is genetically programmed or experience-dependent (Rakic, 1988; O'Leary, 1989). Recent studies have revealed that the early regionalization of the neocortex is primarily determined by gradients of signal molecules and transcriptional factors before thalamocortical projections arrive (Donoghue and Rakic, 1999a, b; Rubenstein, 1999; O'Leary and Nakagawa, 2002; Dufour *et al.*, 2003; Seibt *et al.*, 2003), although interactions between extrinsic factors and thalamocortical projections are suggested to be important in the establishment of a functional architecture (Rakic, 1988; Schlaggar and O'Leary, 1991; Katz and Shatz, 1996; White *et al.*, 2001). Knowledge of the genetic basis of brain architectures, however, is still limited, particularly regarding the genes contributing to functional differences between primate and nonprimate brains (Dorus *et al.*, 2004).

To investigate the evolutionary aspects of areal specification of the primate neocortex, our laboratory have taken the approach of identifying molecular markers that exhibit a highly area- and region-specific expression in the adult primate neocortex (Watakabe *et al.*, 2001a, b; Komatsu *et al.*, 2005). *occl*, the gene encoding the monkey orthologue of follistatin-related protein (*Frp*) and transforming growth factor (TGF)-β1-stimulated clone 36 (*TSC-36*), was identified as a gene preferentially expressed in the monkey visual cortex (Tochitani *et al.* 2001). Nonradioactive *in situ* hybridization (ISH) revealed that *occl* mRNA is particularly abundant in the major thalamocortical recipient layers of the primary visual cortex (V1) (Tochitani *et al.*, 2001; Komatsu *et al.*, 2005), and monocular deprivation markedly downregulates *occl* mRNA expression in adult macaques (Tochitani *et al.*, 2001). Developmentally, the *occl* mRNA expression level is low at birth and markedly increases postnatally (Tochitani *et al.*, 2003). These observations suggest that *occl* mRNA

expression is regulated by the activity of visual afferents from the thalamus and plays a role in activity-dependent plasticity in adult macaque V1.

Comparative neuroanatomy has revealed many differences in the cortical architecture across species. In particular, the sensory cortices of species are specialized in size and organization for adapting to the environment. For example, rodents and some lagomorphs possess ordered multineuronal units called barrels in the primary somatosensory cortex, which represent the topographical organization of connections with the contralateral vibrissae (Woolsey *et al.*, 1975; Wong-Riley and Welt, 1980). Cetaceans communicate by echolocation and have a prominent acoustic system, which is manifested in their enlarged auditory cortices (Revishchin and Garey, 1991; Glezer *et al.*, 1998). The visual cortex is particularly prominent in primates, presumably because diurnal primates greatly depend on vision in their lives. They possess a large and highly organized V1 that has many features not found in other areas or in V1 of other species (Lund *et al.*, 1979; 1994; Rockel *et al.*, 1980; Casagrande and Kaas, 1994).

I thus considered that the abundant expression of *occ1* mRNA in V1 would hold clues to the specific characteristics of the primate visual cortex. In chapter I, I further analyzed detailed features of *occ1* mRNA expression in the adult macaque neocortex, and found two distinguishable modes of *occ1* mRNA expression. In chapter II, I compared expression patterns of *occ1/Frp* (I designate mammalian orthologues of *occ1* other than primates as "*occ1/Frp*" in this thesis) mRNA in the brains of other species, and examined sensory input-dependency of *occ1/Frp* mRNA expression in mouse subcortices.

I found that there were clear differences and similarity in the patterns of *occ1/Frp* mRNA expression among Old World monkeys (macaques), New World monkeys (common marmosets), rodents (mice), lagomorphs (rabbits) and carnivores (ferrets).

Chapter I

Two modes of *occ1* mRNA expression in macaque neocortex

Although *occ1* mRNA is highly abundant in V1 (Tochitani *et al.*, 2001), *occ1* mRNA is also expressed at low levels across other neocortical areas. Because *occ1* mRNA distribution outside of the visual pathways has not yet been well studied (Tochitani *et al.*, 2001; Komatsu *et al.*, 2005), I further analyzed the cortical *occ1* mRNA expression in macaques.

Results

1) *Two distinct modes of* occ1 *mRNA expression in macaque neocortex*

As described previously (Tochitani *et al.*, 2001; Komatsu *et al.*, 2005), *occ1* mRNA signals were most intense in V1 in the macaque neocortex (Fig. I-1 A). Signals were also detected in the middle layers of the extrastriate cortices but progressively more weakly along the ventral visual pathway (Figs. I-1 B-D). The middle temporal area (MT) showed patterns of signals similar to those in V2 (data not shown). The primary somatosensory and auditory cortices also exhibited moderately intense *occ1* mRNA signals in the middle layers, with markedly intense signals that are sparsely distributed in layers IV-VI (Figs. I-1 E, F). There were sparse but intense signals in the motor cortex (Fig. I-1 G). In association cortices (*e.g.*, area 46), sparse signals were observed, but the density of *occ1* mRNA-expressing cells and the intensity of signals were still lower than those in early sensory

and motor cortices (Fig. I-1 H).

Previously, Tochitani *et al.* (2001) reported that both glutamatergic excitatory neurons and GABAergic interneurons express the OCC1 protein in V1. I further examined whether the cell-type specificity of *occ1* expression differs among areas by a double ISH technique using probes for glutamic acid decarboxylase 67 (GAD67) and vesicular glutamate transporter 1 (VGLUT1). GAD67 is a GABA-synthesizing enzyme and a useful marker of GABAergic interneurons (Fitzpatrick *et al.*, 1987; Hendrickson *et al.*, 1994). VGLUT1 is a marker of glutamatergic neurons in the cerebral cortex (Takamori *et al.*, 2000; Fremeau *et al.*, 2001).

Darkfield microscopy images in Figs. I-2 A and B are from macaque V1 sections hybridized with the *occ1* probe and either the VGLUT1 (A) or GAD67 (B) probe. Consistent with our previous report (Tochitani *et al.*, 2001), *occ1* mRNA signals colocalized well with both VGLUT1 and GAD67 mRNA signals. Thus, both glutamatergic excitatory neurons and GABAergic inhibitory interneurons express *occ1* mRNA in V1. *occ1* mRNA signals in layers II-IVCβ overlapped with both VGLUT1 and GAD67 mRNA signals, but the sparse *occ1* mRNA signals in infragranular layers predominantly overlapped with GAD67 mRNA signals, rather than with VGLUT1 mRNA signals. The signals in excitatory neurons were observed in pyramidal-like cells and layer IV spiny stellatelike cells among excitatory neurons in V1. In V2, there were also neurons doubly positive for *occ1*/VGLUT1 mRNA and *occ1*/GAD67 mRNA in layers II-V (Figs. I-2 C, D), but as in V1, sparse *occ1* mRNA signals overlapped particularly with GAD67 mRNA signals in the deeper layers. In the motor cortex, however, the majority of the intense scattered *occ1* mRNA signals colocalized with GAD67 mRNA signals (Fig. I-2 F), and VGLUT1 mRNA signals rarely overlapped with *occ1* mRNA signals (Fig. I-2 E). The intense sparse signals in infragranular layers of the primary somatosensory and primary auditory cortices overlapped with GAD67 mRNA signals, rather than with VGLUT1 mRNA signals, while moderately intense signals in layer III corresponded to both marker signals. Both modes of

occ1/Frp mRNA signals were observed in layer IV (Figs. I-2 G-J). Weak and sparse *occ1* mRNA signals in association areas overlapped mainly with GAD67 mRNA signals (data not shown).

2) *Preferential expression of* occ1 *mRNA in PV-positive subpopulation*

To determine whether *occ1* mRNA is preferentially expressed in a certain subtype of GABAergic interneurons, I performed double ISH to examine the expression of *occ1* mRNA and the three intracellular Ca^{2+}-binding proteins (PV, CB and CR) in the macaque neocortex. My ISH results conserving the areal and laminar distributions of these markers were consistent with those of previously reported immunohistochemical studies (Van Brederode *et al.*, 1990; Kondo *et al.*, 1994; DeFelipe *et al.*, 1999). Photomicrographs in Fig. I-3 show macaque sections hybridized with the *occ1* probe and either the PV probe or the CB probe. In V1, *occ1* mRNA signals coincided well with PV mRNA signals (Fig. I-3 A), but neither with CB mRNA signals (Fig. I-3 B), nor with CR mRNA signals (data not shown). A similar tendency was observed in V2 (Figs. I-3 C, D), the motor cortex (Figs. I-3 E, F), and the somatosensory and auditory cortices (data not shown) in spite of the areal differences in *occ1* mRNA expression. The number of double-positive neurons was counted for each marker in V1, V2 and the motor cortex. Since some pyramidal cells in the primate neocortex are suggested to express certain levels of these Ca^{2+}-binding proteins (Conde *et al.*, 1994; Preuss and Kaas, 1996; Kondo *et al.*, 1999; Ichinohe *et al.*, 2004), I excluded weak signals in pyramidal-like cells from our analysis. I found that 26.9 ± 2.8, 20.8 ± 2.4 and $24.7 \pm 0.5\%$ of GAD67 mRNA-positive cells were *occ1* mRNA-positive in V1, V2 and the motor cortex, respectively (Table I-1). Moreover, in these same areas, 46.7 ± 2.9, 47.5 ± 7.6 and $60.6 \pm 9.3\%$ of PV mRNA-positive cells were also *occ1* mRNA-positive, whereas this was true for only 8.1 ± 1.9, 13.0 ± 6.3 and $8.4 \pm$

2.6% of CB mRNA-positive cells, and for only 0.6 ± 0.3, 1.6 ± 0.5 and 1.2 ± 0.6% of CR mRNA-positive cells (Table I-1). These results suggest that *occ1* mRNA is preferentially expressed in the subpopulation of PV mRNA-positive GABAergic interneurons throughout primate neocortical areas.

3) *Differential effect of monocular deprivation on* occ1 *mRNA expression between two types of neuron in macaque V1*

Tochitani *et al.*, (2001) reported that *occ1* mRNA signal intensity is significantly decreased in layers II-V by monocular deprivation in macaque V1. To determine whether *occ1* mRNA expression in the two populations of excitatory and inhibitory neurons reported above is equally affected by visual deprivation, I carried out double ISH of V1 of macaques monocularly injected with TTX.

Monocular deprivation decreased *occ1* mRNA signal intensity in the deprived columns as reported previously (Fig. I-4 A, Tochitani *et al.*, 2001). Whereas *occ1* mRNA signals in VGLUT1 mRNA-positive cells were strong in the nondeprived column, those in the deprived column were abolished both in pyramidal-like cells and spiny stellatelike cells (Figs. I-4 B, C). Consistent with previous reports that GAD67 expression level of mRNA and cellular PV expression in macaque V1 are not affected by monocular deprivation (Benson *et al.*, 1991; Blümcke *et al.*, 1994), GAD67 and PV mRNA signal intensities were not affected by monocular deprivation in our present study (Fig. I-4 A). In contrast to *occ1* mRNA signals in VGLUT1 mRNA-positive cells, those in GAD67 mRNA- and PV mRNA-positive cells were not significantly different between the nondeprived column and neighboring deprived column (Figs. I-4 D, E). To quantify this observation, I counted the numbers of *occ1*/GAD67 mRNA-positive and *occ1*/PV mRNA-positive neurons in each column

of all layers. This confirmed that the numbers of GAD67 mRNA-positive neurons, PV mRNA-positive neurons, and those double labeled with *occ1* mRNA in deprived columns were not significantly different from those in nondeprived columns (Figs. I-4 F, G). Moreover, the ratios of the number of *occ1*/GAD67 mRNA- or *occ1*/PV mRNA-positive cells to the total number of GAD67 mRNA- or PV mRNA-positive cells in deprived columns did not significantly differ from those in nondeprived columns (nondeprived vs. deprived = $28.7 \pm 2.3\%$ vs. $28.8 \pm 4.3\%$ $p>0.9$ for *occ1*/GAD67, and $40.1 \pm 2.5\%$ vs. $43.6 \pm 2.8\%$ $p>0.2$ for *occ1*/PV mRNA-positive cells, respectively), and were similar to those in untreated V1 (Table I-1).

4) *Pattern of* occ1 *mRNA expression in excitatory neurons corresponds to CO staining pattern*

As shown in Figs. I-1 and I-2, *occ1* mRNA expression in excitatory neurons was mostly restricted to particular layers in sensory cortices in the macaque neocortex. In V1, layer IVC exhibited the strongest *occ1* mRNA expression, although the signals in excitatory neurons were also observed in layers II, III, IVA and less prominently in layer IVB. Deeper layer III and layer IV of extrastriate cortices, and the middle layers of the primary somatosensory and auditory areas also showed *occ1* mRNA signals in excitatory neurons. The distribution pattern of excitatory neurons expressing *occ1* mRNA corresponded well to the laminar-specific CO staining pattern (Fig. I-5). I further noted a bloblike distribution of *occ1* mRNA signals in layers II/III in V1 (see Fig. I-1 A). This signal distribution corresponds to blobs in a tangential section in layer III of V1, as verified by comparing with an adjacent CO-stained section (Fig. I-6).

Discussion

In this chapter, I analyzed the expression patterns of *occl/Frp* mRNA in the neocortices of macaques. In the macaque neocortex, I found i) a conspicuous, activity-dependent *occl* mRNA expression in excitatory, but not GABAergic neurons in infragranular and granular layers of V1, ii) a moderately strong *occl* mRNA expression in excitatory neurons in the middle layers of primary somatosensory, auditory, and extrastriate visual cortices, and iii) *occl* mRNA expression in GABAergic (particularly PV-positive) interneurons throughout the neocortex. The distribution of excitatory neurons expressing *occl* mRNA corresponded well with the distribution of CO activity in sensory areas. In this section, I consider the functional roles of OCC1 especially in V1, and the meaning of cell type specificity and area-difference of *occl* mRNA expression.

1) *Function of* OCC1 *in macaque brain*

OCC1/FRP is a secretable glycoprotein and considered to belong to the secreted protein acidic and rich in cystein (SPARC)/BM-40 family, which shares one follistatin-like (FS) domain followed by one extracellular Ca^{2+}-binding (EC) domain (Hohenester *et al.*, 1997; Yan and Sage, 1999). The FS domain is a cystein-rich domain, in which all the cystein residues are disulfide-bonded, and is homologous to follistatin and Kazal-type protease inhibitors. The EC domain is largely α-helical and contains a canonical pair of EF-hands, with high-affinity Ca^{2+}-binding sites (Engel *et al.*, 1987; Hohenester *et al.*, 1997). This family is composed of SPARC/BM-40, SC1/hevin, QR1, testicans and SMOCs, as well as OCC1/FRP (Yan and Sage, 1999; Vannahme *et al.*, 2003).

OCC1/FRP may be a multifunctional protein, because *occ1/Frp* mRNA is strongly expressed in most human tissues as determined by Northern hybridization analysis (Tanaka *et al.*, 1998; Vertegaal *et al.*, 2000), and genes of this family are mostly multifunctional (Yan and Sage, 1999). Although the physiological function of OCC1/FRP in the brain remains to be elucidated, I can suggest a couple of possible roles of OCC1/FRP.

OCC1/FRP may interact with some extracellular growth factors (neurotrophic factor) or may act as a trophic factor itself and thereby regulate the neuronal phenotype. *occ1/Frp* was first identified as a gene whose expression is stimulated by TGF-β1 in mouse osteoblastoma cell lines (Shibanuma *et al.*, 1993). Although Zwijsen *et al.* (1994) reported that OCC1/FRP does not inhibit the function of TGF-β1 in feedback signaling, follistatin and FSTL3, which have three or two FS domains, bind to some members of the TGF-β family and suppress their activities (Nakamura *et al.*, 1990; Tsuchida *et al.*, 2000). Thus, secreted OCC1/FRP could control the function of molecules similarly to TGF-β.

Alternatively, OCC1/FRP may interact with the extracellular matrix (ECM). Recent studies have suggested that ECM has important roles in activity-dependent synaptogenesis and plasticity both in developing and adult brains (Dzwonek *et al.*, 2004; Pavlov *et al.*, 2004). One major component of ECM is chondroitin sulphate proteoglycans (CSPGs), some of which can be recognized by the Cat-301 antibody (Zaremba *et al.*, 1989) and which inhibit axonal sprouting (Fitch and Silver, 1997; Fawcett and Asher, 1999). Pizzorusso *et al.* (2002) demonstrated that the degeneration of CSPGs reactivates visual plasticity in the adult rat visual cortex, showing that CSPGs inhibit neuronal remodeling in the adult brain. Some members of the SPARC/BM-40 family were suggested to promote cell-to-ECM interactions. SPARC/BM-40 and SC1/hevin are ECM glycoproteins and participate in the regulation of morphogenesis and cellular differentiation through the modulation of cell-matrix interactions (Tremble *et al.*, 1993; Mendis and Brown, 1994; Mendis *et al.*, 1994; Yan and Sage, 1999; Brekken *et al.*, 2003). Testicans, which are abundantly expressed in the brain as

Ca^{2+}-binding proteoglycans (Vannahme *et al.*, 1999), inhibit neurite extension from cultured neurons (Marr and Edgell, 2003; Schnepp *et al.*, 2005). Furthermore, OCC1/FRP has been suggested to have inhibitory effect on ECM degeneration, such as an inhibition of invasion of tumor cells and downregulation of matrix metalloproteinases expression (Johnston *et al.*, 2000; Tanaka *et al.*, 2003). Therefore, OCC1 could stabilize neuronal connections by stabilizing ECM, resulting in decreased plasticity in V1 and other early sensory cortices that express *occ1* in adult primates. If this is the case, the downregulation of *occ1* mRNA expression in the absence of neuronal activity may stimulate the reorganization of neuronal connections.

2) *Cell-type specificity and region specificity of* occ1/Frp *mRNA expression*

In the present study, we demonstrated that *occ1* mRNA is expressed both in excitatory neurons and GABAergic inhibitory interneurons in the macaque cerebral cortex. Excitatory neurons mostly consist of spiny stellate cells distributed in layer IV of the primary sensory areas, and pyramidal cells distributed in the supra- and infragranular layers throughout the neocortex (McCormick *et al.*, 1985; DeFelipe and Farinas, 1992; Nieuwenhuys, 1994). As determined from their location and morphology, *occ1* mRNA appears to be expressed in both types of excitatory neuron.

I also demonstrated that *occ1* mRNA is preferentially expressed in PV-positive subtypes among interneurons in macaques. According to the data obtained by previous research, PV-, CB-, and CR-positive cortical neuronal subpopulations are mostly GABAergic inhibitory interneurons, and are associated with distinct morphological and electrical properties (Van Brederode *et al.*, 1990; DeFelipe, 1997; Kawaguchi and Kubota, 1997; Markram *et al.*, 2004; Zaitsev *et al.*, 2005). These subtypes are also associated with expressions of other genes, such as neuropeptides (Kawaguchi and

Kubota, 1997), ion channels (Sekirnjak *et al.*, 1997; Chow *et al.*, 1999), AMPA receptors (Kondo *et al.*, 1997) and trkB receptors (Cellerino *et al.*, 1996). Subsets of these molecules are suggested to contribute to the morphological and electrical properties of GABAergic neuronal subtypes (Toledo-Rodriguez *et al.*, 2004). It remains, however, to be studied how the function of OCC1 is related to the functions of these genes that have the unique properties in PV-positive interneurons.

PV-positive GABAergic interneurons are mostly basket cells that innervate the somas of pyramidal cells, or chandelier cells that innervate the axon initial segment of pyramidal cells with a strong inhibitory effect on these cells (Williams *et al.*, 1992; Conde *et al.*, 1994; Markram *et al.*, 2004). Both types of cell occasionally express CB in the rat somatosensory cortex (Wang *et al.*, 2002). These reports may be consistent with our data that 8-13% of CB-positive cells express *occ1* mRNA in the macaque neocortex (see Table 1), if we assume that parts of basket and chandelier cells also express CB in macaques.

Expression of *occ1/Frp* mRNA shows areal differences within the PV-positive population as follows. i) *occ1* mRNA is expressed only in 46-60% of PV-positive cells in areas examined, ii) *occ1* mRNA expression in PV-positive neurons seems most strong in the sensorimotor cortex and least strong in association areas in macaques.

I illustrated that the distribution of excitatory neurons expressing *occ1* mRNA corresponded to CO activity. A high CO activity is generally related to prominent neuronal activity derived by thalamocortical inputs into sensory cortices (Wong-Riley, 1979; Wong-Riley and Welt, 1980). CO blobs in layers II/III of macaque V1 receive projections from koniocellular layers in the dLGN (Livingstone and Hubel, 1982; Ding and Casagrande, 1998). Taken together with the observation that *occ1* mRNA expression in excitatory neurons of V1 is strongly regulated by retinal projection, the significant correspondence between *occ1* mRNA expression and CO activity implies that excitatory neurons express *occ1* mRNA in response to strong neuronal activity throughout the

sensory cortices in macaques. However, it seems that the excitatory neurons of V1 uniquely possess a distinct genetic program for expressing particularly abundant *occ1* mRNA in an activity-dependent manner, since the *occ1* mRNA expression was much more prominent in V1 than in other sensory areas: *occ1* mRNA expression in the primary somatosensory and auditory cortices was much weaker than that in V1, while CO activity in these areas was strong (see Fig. 5, Jones and Friedman, 1982; Jones et al., 1995). It is therefore suggested that both the genetic program and sensory input are important to determine the characteristic pattern of *occ1* mRNA expression in primate V1. Further studies on the mechanisms underlying this activity-dependent regulation of *occ1* mRNA expression will elucidate molecular characteristics underlying the formation of cortical architecture.

Figures and Table

Figure I-1

Coronal sections for ISH of *occ1* (right panels) and adjacent Nissl-stained sections (left panels) of macaque neocortex. A: primary visual cortex (V1), B: secondary visual area (V2), C; occipital temporal cortex (TEO), D: temporal cortex (TE), E: primary somatosensory cortex (area 3b), F: primary auditory cortex (A1), G: primary motor cortex (area 4), H: prefrontal association cortex (area 46). Scale bar in A = 300 μm.

Figure I-2

Coronal sections of macaque V1 (A, B), V2 (C, D), area 4 (E, F), area 3b (G, H) or A1 (I, J) for double ISH of *occ1* (red) and either VGLUT1 (A, C, E, G, I) or GAD67 (B, D, F, H, J) (green). Scale bar = 150 μm.

Figure I-3

Coronal sections of macaque V1 (A, B), V2, (C, D) or area 4 (E, F) for double ISH of *occ1* (red) and either PV (A, C, E) or CB (B, D, F) (green). Scale bar = 150 μm.

Figure I-4

A: Coronal section of monocularly deprived macaque V1 for double ISH of *occ1* (red) and PV (green) (the survival time after deprivation was 10 days). Scale bar = 300 μm. N/nondeprived column, D/deprived column

B-E: Highly magnified sections of monocularly deprived macaque V1 in layer IVCβ with survival time of 14 days for double ISH. Sections were hybridized with the *occ1* probe (red) and either the VGLUT1 (B, C) or PV (D, E) probe (green). B and D depict cells in the nondeprived columns and C and E in the neighboring deprived columns. Arrows indicate cells that showed VGLUT1 mRNA signals. Circles indicate cells that showed PV mRNA signals. Scale bar in B = 50 μm. F and G represent the normalized numbers (/mm^2) of interneuron marker-positive cells and double-positive cells with *occ1* mRNA in both deprived and nondeprived columns of monocularly deprived macaque V1 (n = 4) (F: with GAD67, G: with PV). Each mean±S.E.M in the nondeprived columns and deprived columns are compared. *p* values are presented over each bar.

Figure I-5

Coronal sections for ISH of *occ1* (B, E, H) and adjacent Nissl-stained (A, D, G) and CO-stained sections (C, F, I) of macaque visual cortex (A-C), sensorimotor cortex (D-F) or primary auditory cortex (G-I). Upper is dorsal and right is medial. Arrows indicate V1/V2 borders. Scale bar = 1.0 mm. ca/calcarine sulcus, cs/central sulcus, lf/lateral fissure

Figure I-6

Tangential section for ISH of *occ1* (A) and adjacent section visualized for CO activity (B) in layer III of normal macaque V1. Arrowheads indicate the same blood vessels for each section. Scale bar = 500 μm.

Table I-1

Statistics of double ISH of several areas in macaques and ferrets. The numbers of cells that exhibit signals of each GABAergic marker (/mm^2), the numbers of cells that exhibit double-positive signals for marker and *occ1/Frp* (/mm^2), and the number ratios of double-positive and marker-positive cells are shown. The values are means ± S.E.M for three individuals.

Figure I-1

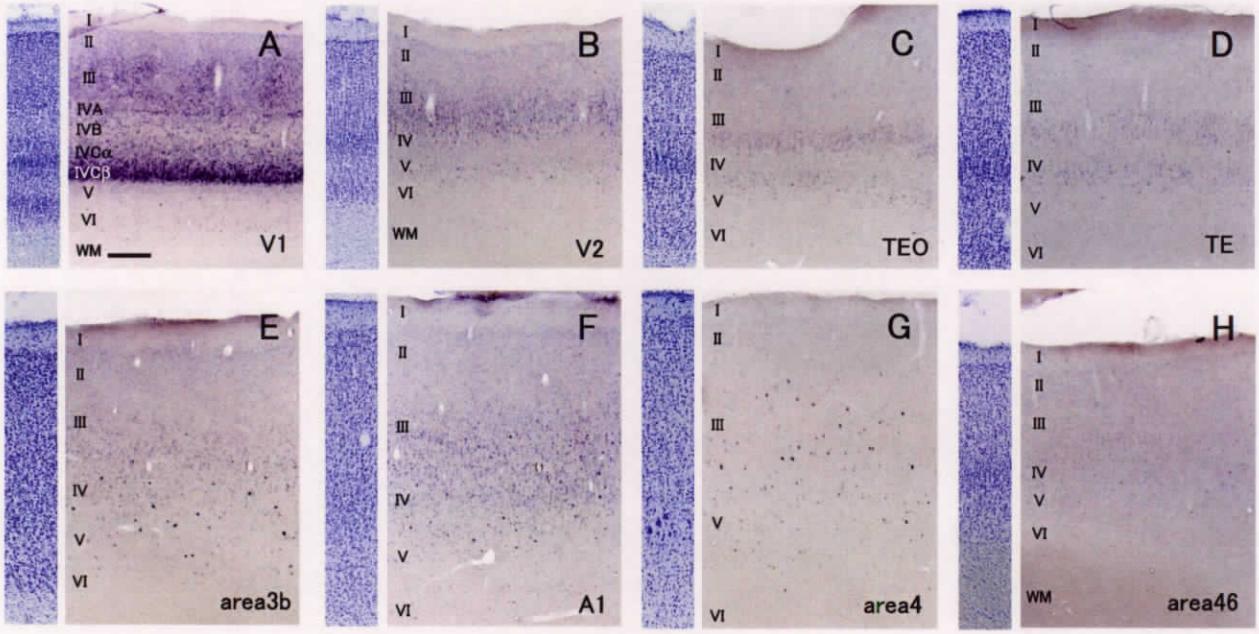
A
I
II
III
IVA
IVB
IVCα
IVCβ
V
VI
WM
V1
B
I
II
III
IV
V
VI
WM
V2
C
I
II
III
IV
V
VI
TEO
D
I
II
III
IV
V
VI
TE
E
I
II
III
IV
V
VI
area3b
F
I
II
III
IV
V
VI
A1
G
I
II
III
V
VI
area4
H
I
II
III
IV
V
VI
WM
area46

Figure I-2

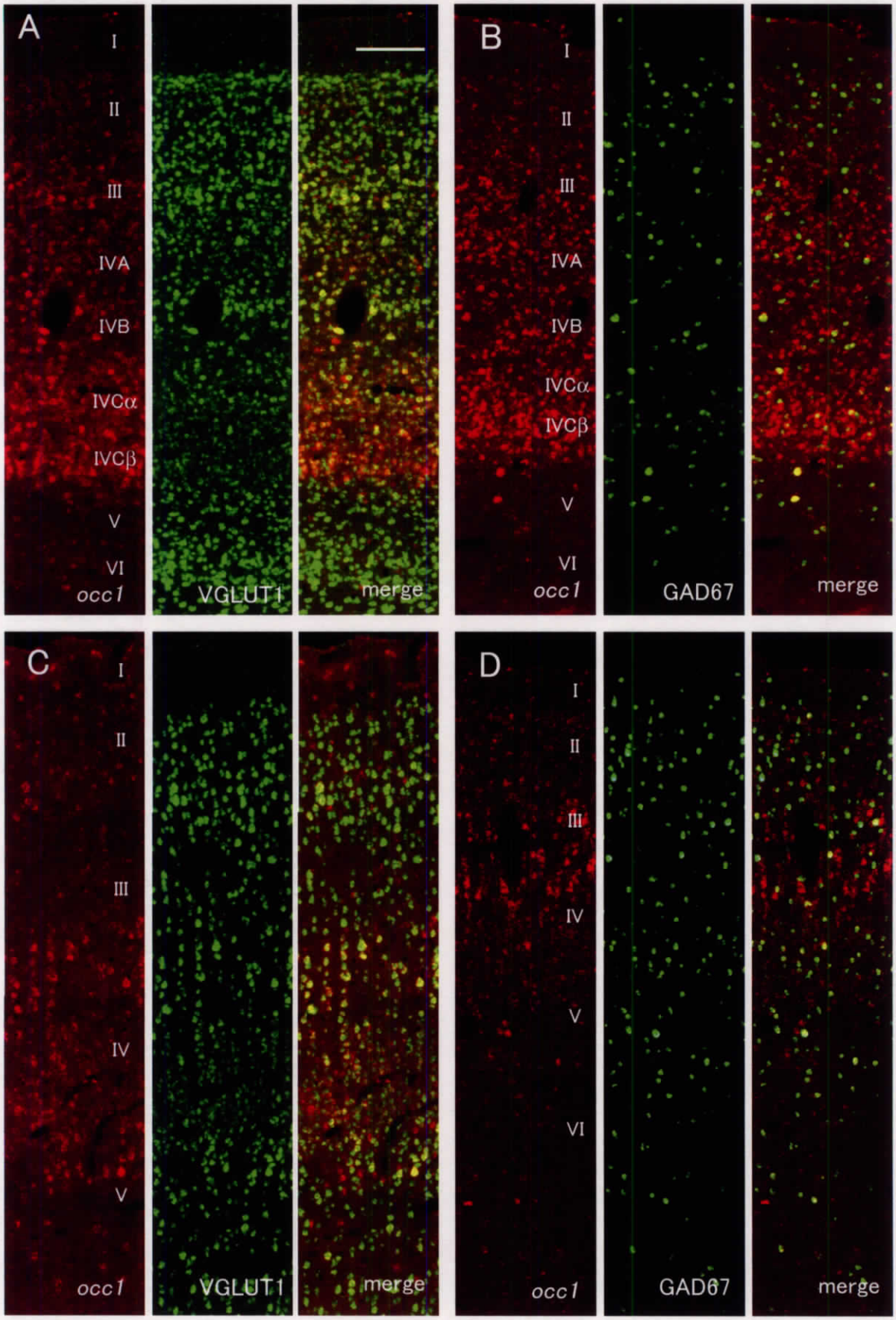
A
I
II
III
IVA
IVB
IVCα
IVCβ
V
VI
occ1
VGLUT1
merge
B
I
II
III
IVA
IVB
IVCα
IVCβ
V
VI
occ1
GAD67
merge
C
I
II
III
IV
V
occ1
VGLUT1
merge
D
I
II
III
IV
V
VI
occ1
GAD67
merge

Figure I-2 continuation 1

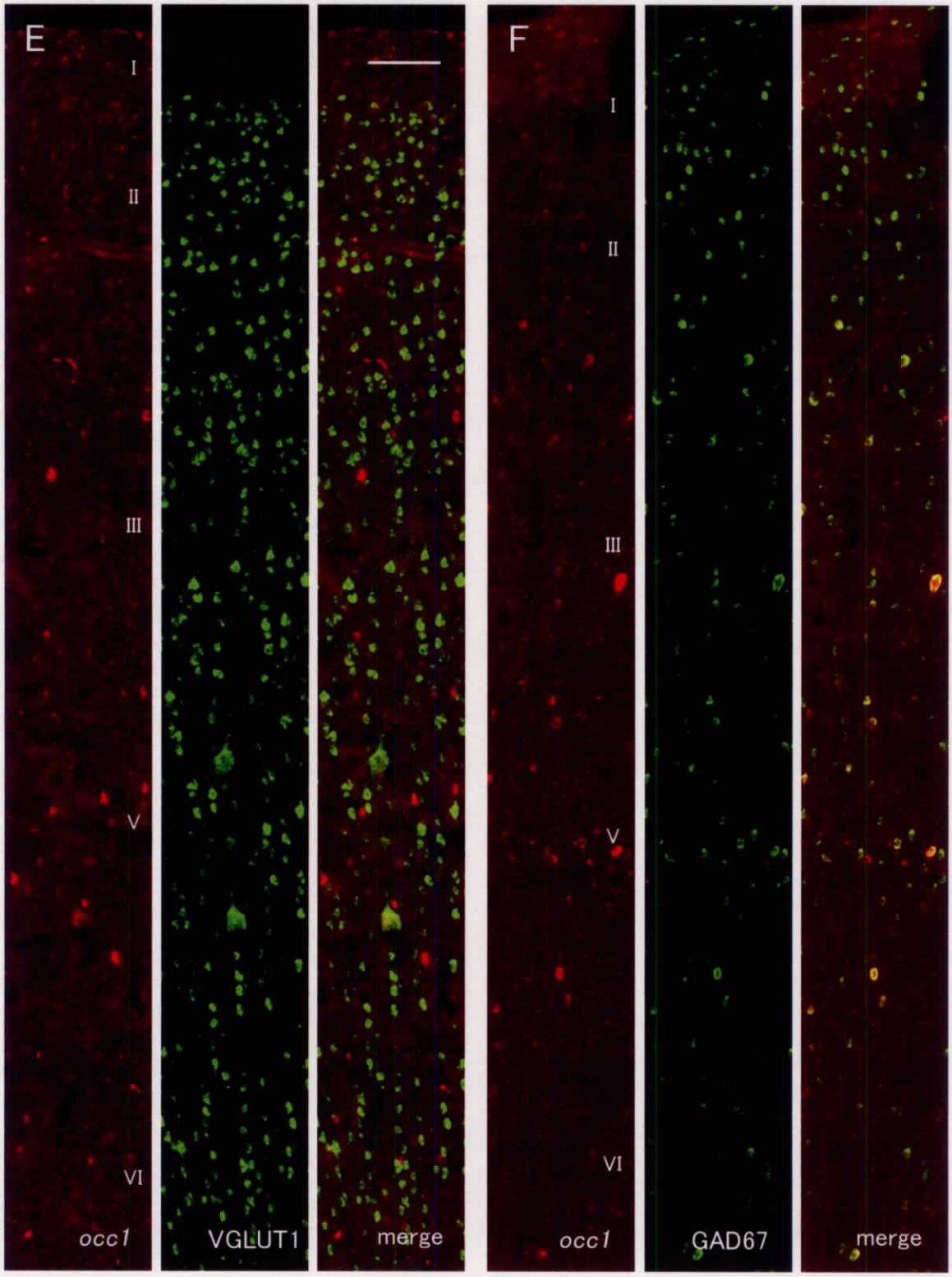

Figure I-2 continuation 2

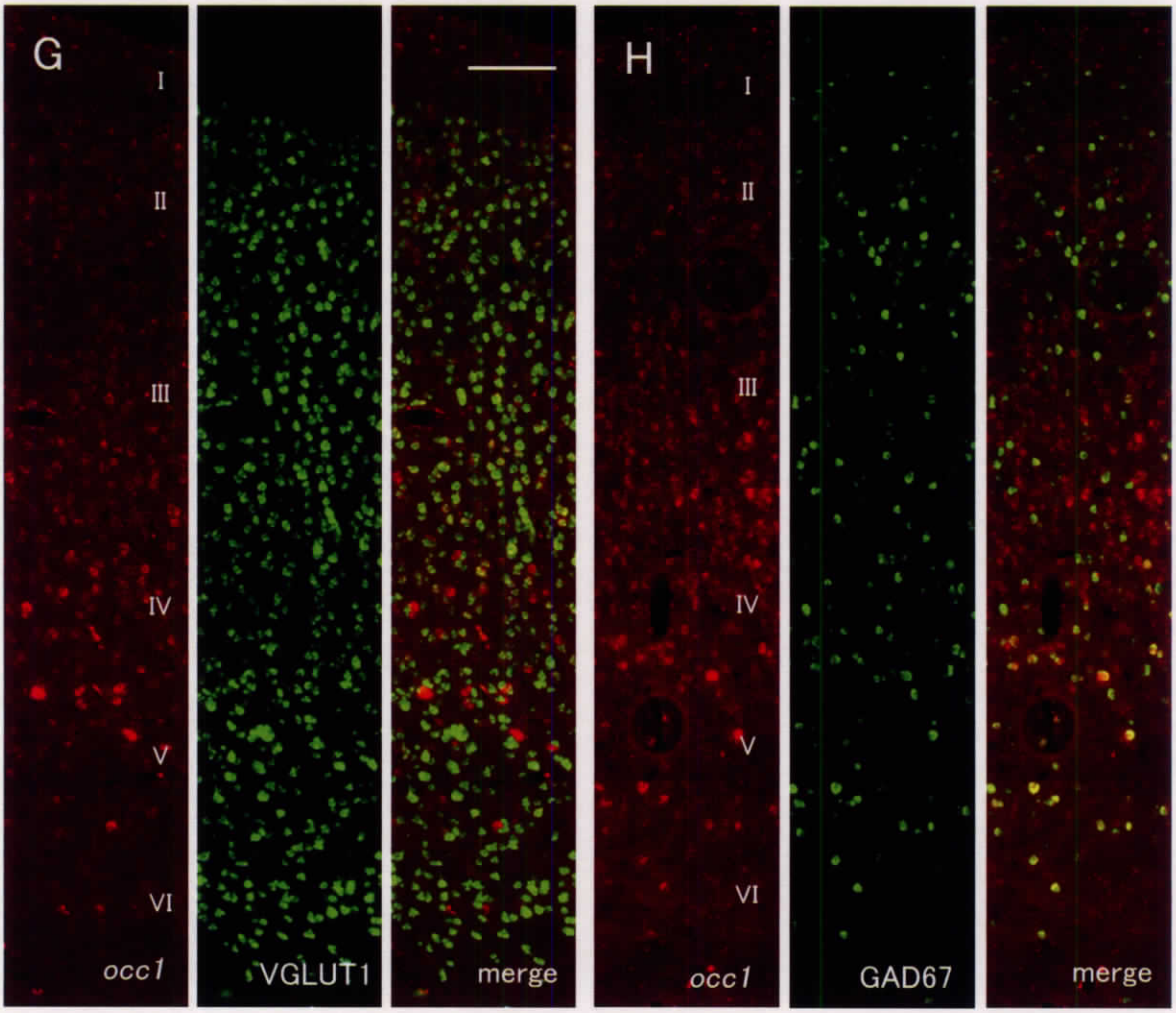

Figure I-2 continuation 3

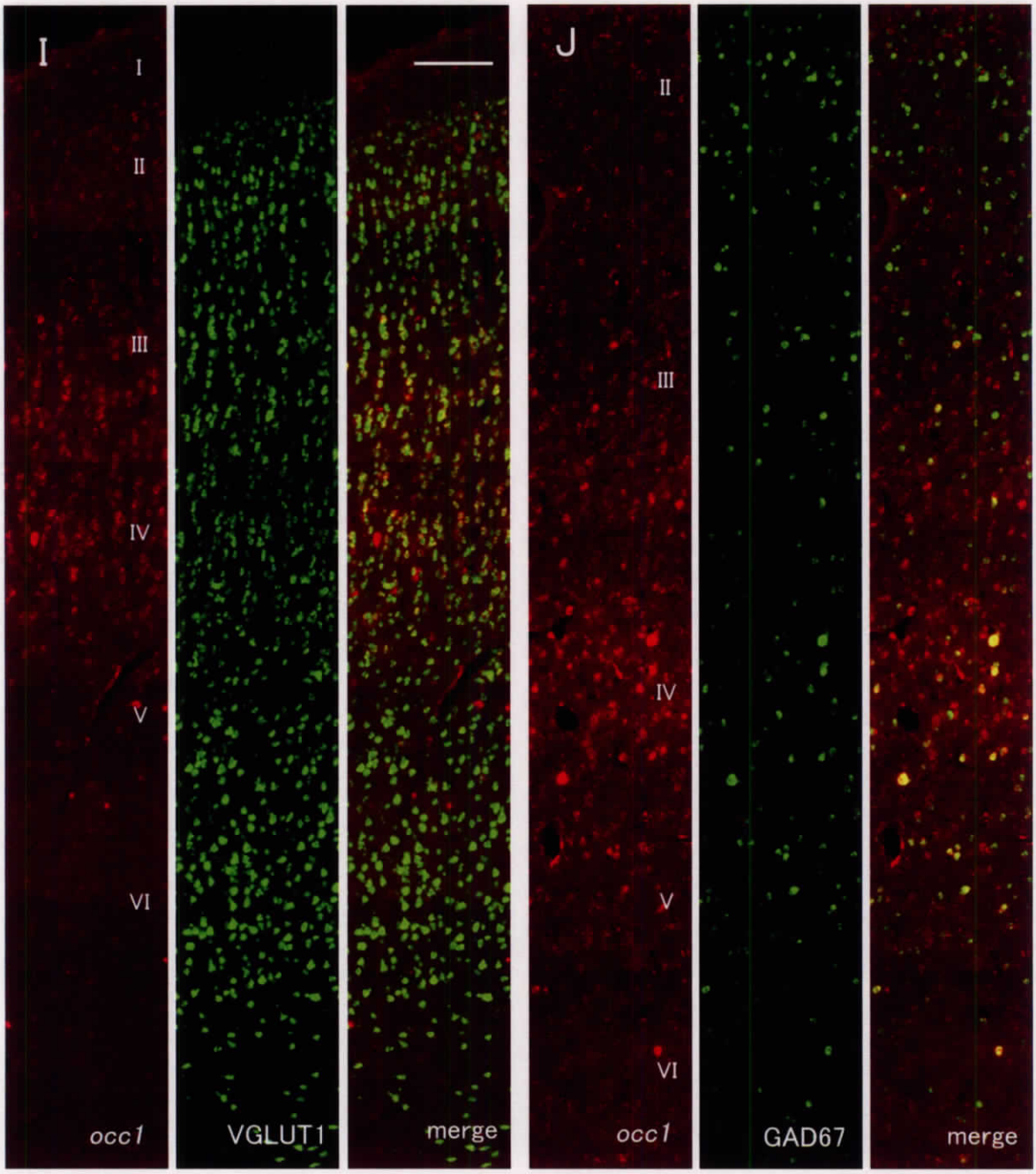

Figure I-3

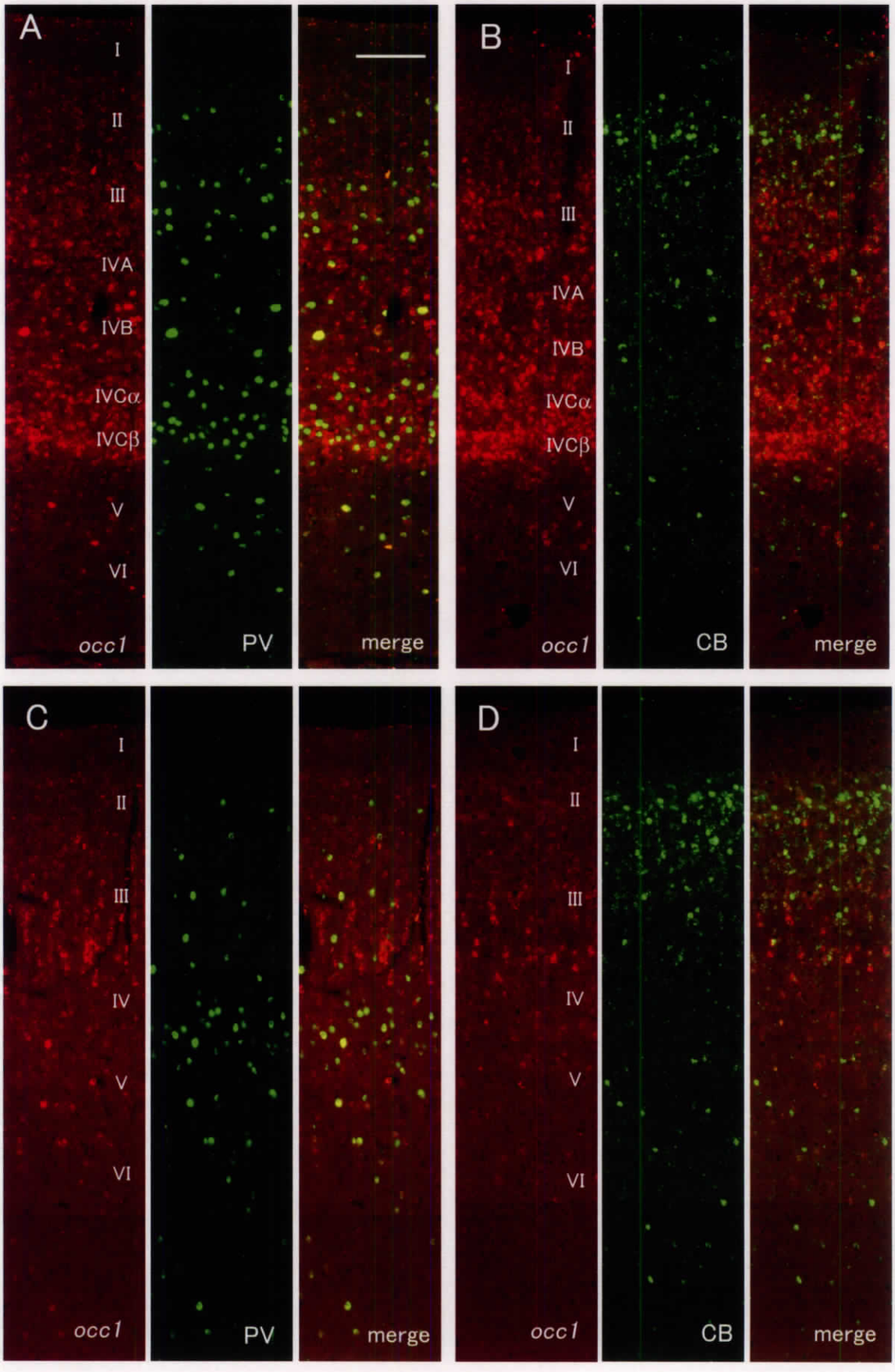
A
I
II
III
IVA
IVB
IVCα
IVCβ
V
VI
occ1
PV
merge
B
I
II
III
IVA
IVB
IVCα
IVCβ
V
VI
occ1
CB
merge
C
I
II
III
IV
V
VI
occ1
PV
merge
D
I
II
III
IV
V
VI
occ1
CB
merge

Figure I-3 continuation 1

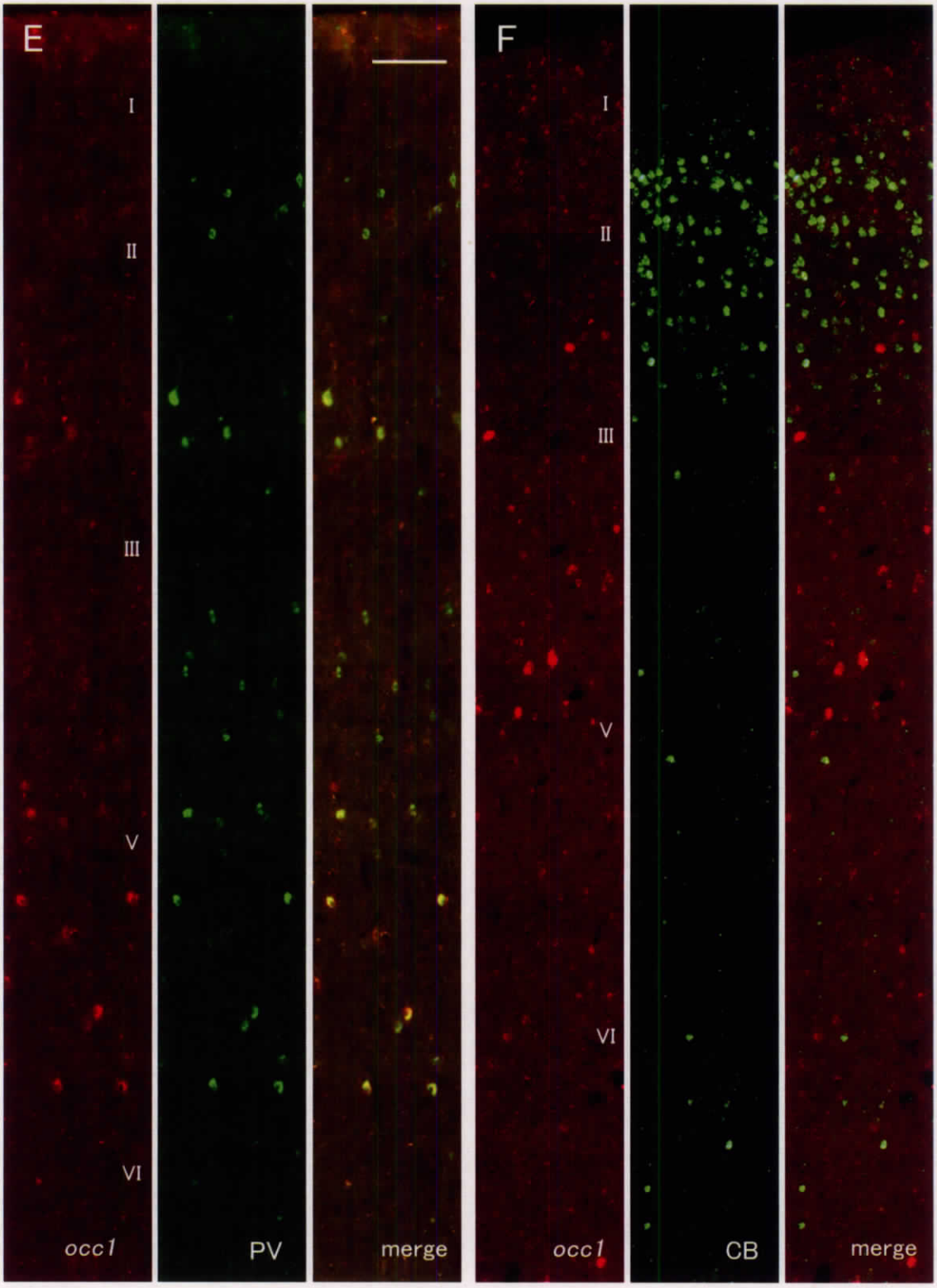

Figure I-4

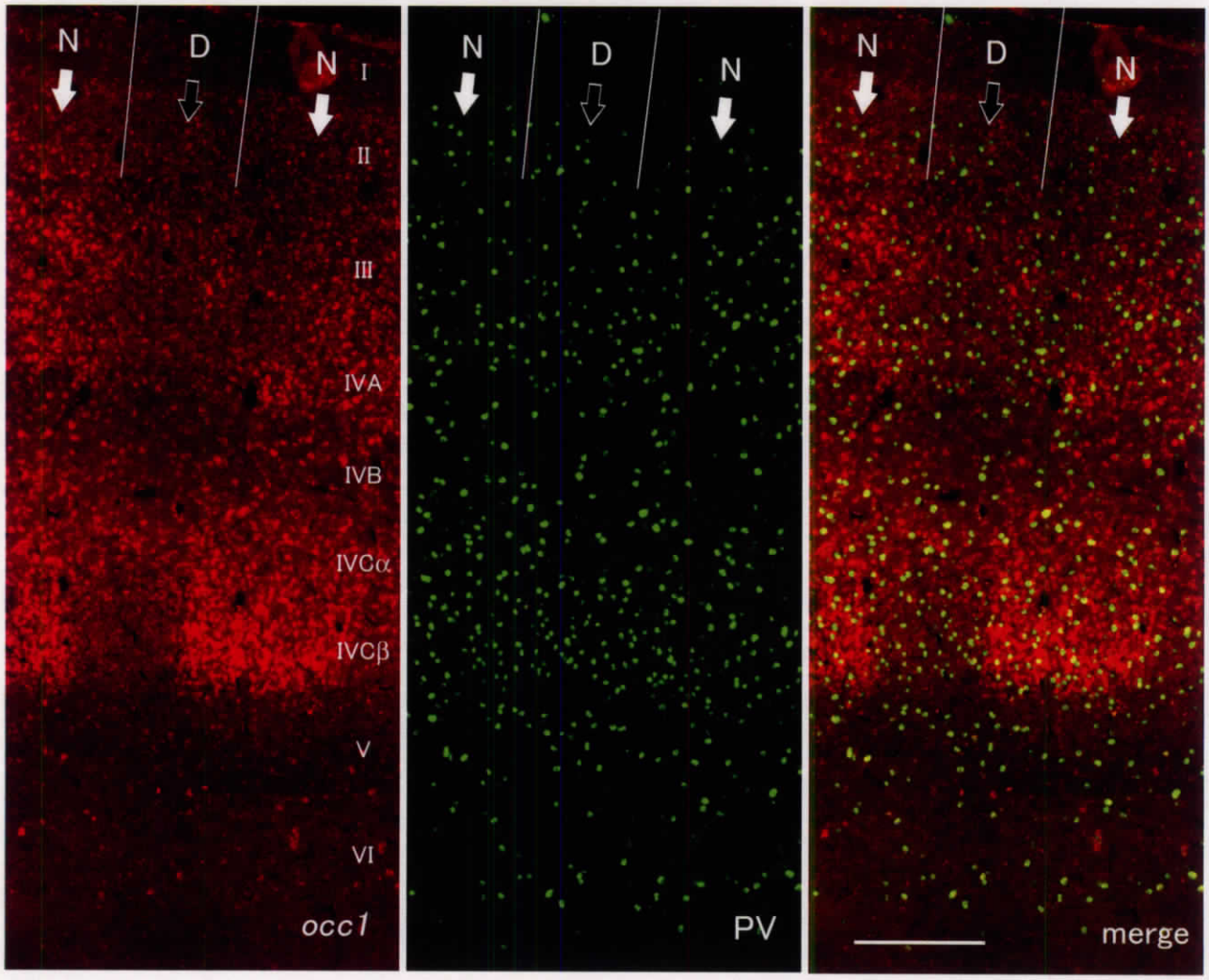

Figure I-4 continuation 1

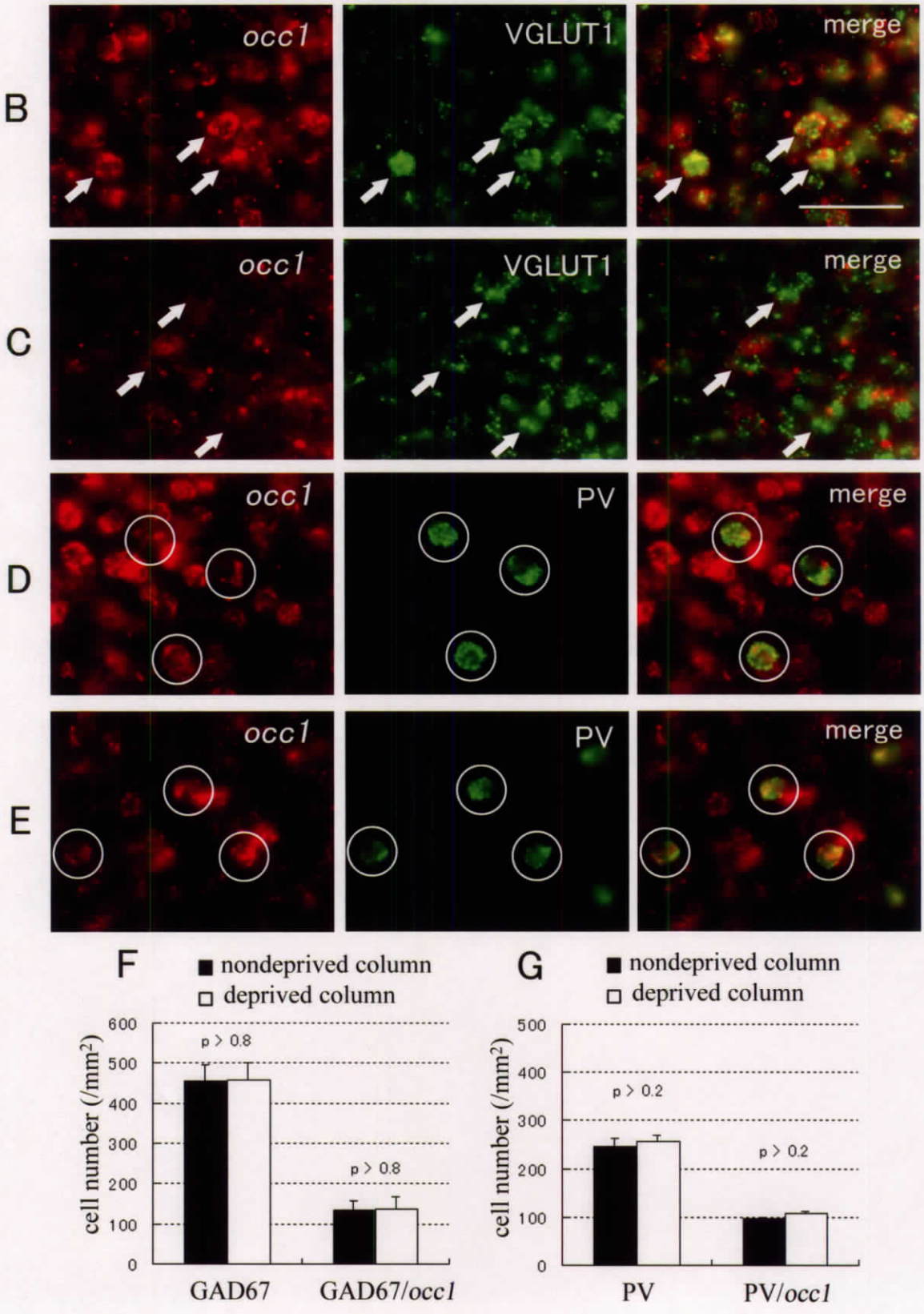

Figure I-5

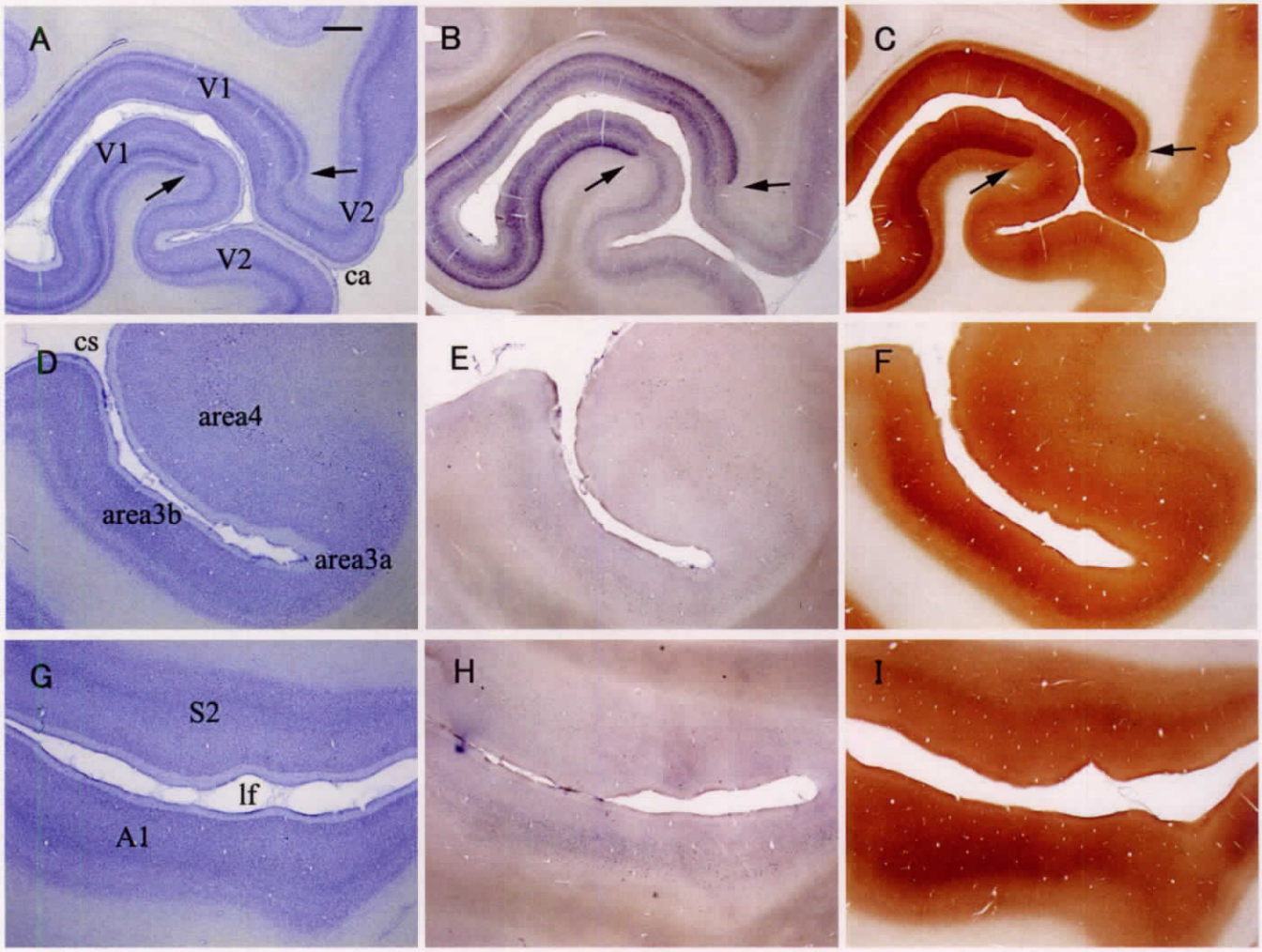

Figure I-6

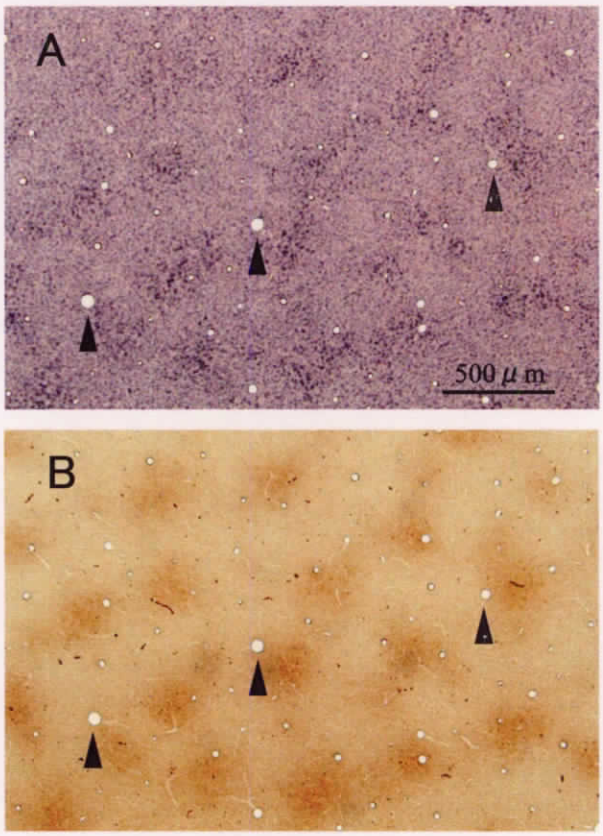

Table I-1

Macaque V1

	Marker (/mm^2)	Double-positive (/mm^2)	%
GAD67	400.7±38.4	106.7±11.7	26.9±2.8
PV	204.6±15.8	96.1±11.4	46.7±2.9
CB	63.6±7.8	5.3±1.4	8.1±1.9
CR	40.9±5.7	0.6±0.3	1.6±0.7

Macaque V2

	Marker (/mm^2)	Double-positive (/mm^2)	%
GAD67	328.7±17.1	67.1±4.8	20.8±2.4
PV	57.5±16.4	24.9±4.2	47.5±7.6
CB	66.1±18.1	7.1±2.9	13.0±6.3
CR	65.7±10.3	1.6±0.5	3.1±1.5

Macaque motor

	Marker (/mm^2)	Double-positive (/mm^2)	%
GAD67	200.3±15.1	49.4±3.5	24.7±0.5
PV	40.1±10.1	23.5±5.0	60.6±9.3
CB	69.6±16.3	4.7±0.7	8.4±2.6
CR	43.7±4.6	1.2±0.6	2.9±1.4

Ferret V1

	Marker (/mm^2)	Double-positive (/mm^2)	%
GAD67	211.2±38.6	72.4±15.4	36.7±8.7
PV	95.3±13.6	57.5±3.3	64.7±11.0
CB	10.9±4.2	1.8±0.6	18.4±1.2
CR	22.3±6.0	1.1±0.4	5.6±3.0

Chapter II

Interspecies comparison of *occ1/Frp* mRNA expression

The primary visual area is highly specialized in primates with massive thalamocortical inputs (Hubel and Wiesel, 1972). In contrast, most nonprimate mammalian species depend more on nonvisual or multimodal senses, and the organization of neurons and patterns of neuronal activity in their cortices are highly diversified (Kaas, 1989). Therefore, the preferential *occ1/Frp* mRNA expression in V1 could be restricted to primates. To clarify this point, I examined *occ1/Frp* mRNA expression patterns in the brains of marmosets, mice, rabbits and ferrets, as well as macaques.

Results

1) occ1/Frp *mRNA distribution in other mammalian neocortices*

In a low magnification of sagittal sections of each species, I could find strong *occ1* mRNA signals in marmoset V1 although not as prominent as in macaque V1 (Fig. II-1 A). Area-selective *occ1/Frp* mRNA signals like those in macaque and marmoset V1 were, however, not observed in the cortex of other species, whereas strong *occ1/Frp* mRNA signals could be seen in the hippocampus and some other subcortical regions (Fig. II-1 B-D).

Although the marmoset is a phylogenetically distant primate from the macaque, the V1 structure is relatively well conserved between New and Old World monkeys (Spatz *et al.*, 1994; Krubitzer,

1995). Strong laminar-specific *occ1* mRNA signals were observed, which were not observed in the case of using the control sense probe in layer IVC in marmoset V1 (Figs. II-2 B, E, F). The distribution pattern of these signals corresponded well with dense CO staining in layer IVC (Fig. II-2 C). Layers II and III also showed *occ1* mRNA signals. However, the *occ1* mRNA expression in the somatosensory, auditory and extrastriate visual areas in marmosets was not as specific to the thalamocortical recipient layers as in macaques: that is, moderately intense signals were observed throughout the layers with slightly intense signals in the superficial layers. The pattern was similar to that in the motor area. Although data from a double ISH was not available, the diffuse distribution of *occ1* mRNA signals is consistent with the existence of GABAergic interneurons in these areas (Fitzpatrick *et al.*, 1987) (Figs. II-2 B, H). Higher association areas showed weaker signals than any other areas (data not shown).

In mouse V1, only weak signals were observed except for some cells in deeper layer VI with moderately intense signals (Fig. II-3 B). In the rabbit visual cortex, weak signals were observed in the upper part of layer V, and neurons in layers II and III were also weakly stained. Some cells, which were presumably interneurons and showed intense signals, were sparsely observed in all layers (Fig. II-3 F). Unlike in primates, area-specific differences in *occ1/Frp* mRNA expression were not pronounced either in mice or rabbits, even in the barrel field that receives strong thalamocortical inputs (Fig. II-3 D, Wong-Riley and Welt, 1980). In the ferret visual cortex, laminar-specific signals were not observed. *occ1/Frp* mRNA signals were sparsely distributed in all layers (Fig. II-3 J), which appeared to be in interneurons. These signals were most abundant in the caudal, visual cortex, both in terms of cell number and signal intensity, and signal intensity gradually decreased toward the rostral, frontal cortex (Fig. II-3 H).

Double ISH revealed that most of the sparsely distributed signals in the ferret visual cortex overlapped with GAD67 mRNA signals, being consistent with our interpretation that these signals

were in GABAergic interneurons (data not shown). Further analysis demonstrated that these signals were most frequently detected in PV mRNA-positive GABAergic interneurons, rather than in CB or CR mRNA-positive neurons, as similarly observed in macaques (Fig. II-4 A, B and Table I-1). Scattered signals in rabbits also overlapped with GAD67 mRNA signals, but in this species, these scattered signals were evenly observed in all three GABAergic subtypes (Fig. II-4 C, D).

2) *Subcortical expression of* occ1/Frp *mRNA in macaques and mice*

In addition to *occ1* mRNA signals in neocortices, I detected many intense signals in the subcortical regions of each species. To determine whether the subcortical expression pattern is conserved, I compared *occ1/Frp* mRNA expression patterns between macaques and mice in more detail.

As summarized in Table II-1, we found several similar patterns of expression in the subcortical nuclei in macaques and mice. For example, both species showed strong signals in the glutamatergic cells of the lower auditory and vestibular relay nuclei (e.g., ventral cochlear nucleus and vestibular nuclei; Figs. II-5 J, K and Fig. II-6 J), lower somatosensory relay nuclei (e.g., external cuniate nucleus and gracil nucleus) and motor relay nuclei (e.g., facial nucleus and hypoglossal nucleus; Figs. II-5 I, K and Figs. II-6 I, K), although one of the auditory relay nuclei, the superior olivary nucleus, showed much weaker signals in mice than in macaques (Fig. II-5 G and Fig. II-6 G). In contrast, we observed very few signals in the cholinergic or adrenergic autonomic nerve systems such as the locus coeruleus and dorsal motor nucleus of vagus in both species (Figs. II-5 H, K and Figs. II-6 H, K). In dopaminergic and serotonergic nuclei such as the substantia nigra, dorsal raphe and median raphe, signal intensity varied among nuclei, even within a nucleus (Fig. II-5 E and Fig.

II-6 E). In the cerebellum, weak signals, which seem to correspond to Bergman glias, were observed in Purkinje layers both in macaques and mice (Fig. II-5 L and Fig. II-6 L).

However, there were also notable differences in some nuclei. Although I did not observe any strong signals in the macaque thalamic nuclei, there were strong signals in the mouse thalamic nuclei, particularly in the anterior part (Fig. II-5 D and Fig. II-6 D). While only weak signals were detected in the magnocellular layers in macaque dLGN (Tochitani et al. 2001), I detected strong signals in most of the cells in mouse dLGN (Fig. II-7 A). Although pyramidal cells in CA2 were selectively labeled in the macaque hippocampus (Tochitani et al. 2003, Fig. II-5 A), pyramidal cells in CA1-CA4 and granule cells in dentate gyrus were uniformly labeled in mice (Fig. II-6 A). Although we observed no signals in macaque Islands of Calleja (ICj), strong signals were observed in mouse ICj (Fig. II-5 C and Fig. II-6 C). Precerebellar nuclei showed marked differences in signals between macaques and mice. While macaques showed relatively weak signals in the pontine nuclei, reticulotegmental nucleus, inferior olivary nucleus and cerebellar nuclei ($\pm$, +, - and $\pm$ respectively), mice showed strong signals in these areas (++, ++, $\pm$ and ++, respectively) (Fig. II-5 F and Fig. II-6 F).

Despite some of these marked differences, I also found notable similarities in the subcortical *occl/Frp* mRNA expression pattern between macaques and mice (see ☆☆ and ☆ in Table II-1), suggesting that the products play some conserved roles in the subcortical nuclei.

3) *Examination of sensory input dependence of* occl/Frp *mRNA expression in mouse subcortex*

I found above that *occl/Frp* mRNA was strongly expressed in the sensory relay nuclei in the mouse subcortex. Because sensory relay nuclei mostly consist of excitatory projection neurons,

occ1/Frp mRNA expression in the sensory relay nuclei of mice might be regulated by sensory activity as well. To examine this possibility, I determined the effects of sensory deprivation on *occ1/Frp* mRNA expression in the sensory relay nuclei in adult mice.

I examined *occ1/Frp* mRNA expression in the dLGN of monocularly deprived mice. As reported for rats (Land, 1987), two weeks of monocular deprivation of adult mice resulted in a decrease in CO activity in the dLGN domains innervated by the enucleated eye (monocular region of the dLGN contralateral to the enucleated eye and binocular regions of both dLGNs) (Figs. II-7 G, H). However, *occ1/Frp* mRNA signals were not affected by the same treatment (Figs. II-7 E, F). *occ1/Frp* mRNA expression in the mouse visual cortex was also not affected (data not shown). Binocular deprivation similarly had little effect on *occ1/Frp* mRNA expression (Fig. II-7 B), although CO activity decreased (Fig. II-7 D). These results suggest that *occ1/Frp* mRNA expression in the mouse dLGN is not significantly regulated by sensory activity, unlike in macaque V1.

Unilateral cochleotomy was conducted to induce auditory deprivation in adult. Auditory inputs are relayed from the ipsilateral cochlear nucleus without inputs to the contralateral cochlear nucleus. As reported previously (Illing 2001), a 7-day cochleotomy stimulated the expression of GAP43 in the ipsilateral anteroventral cochlear nucleus (Figs. II-8 C, D). However, it did not significantly affect *occ1/Frp* mRNA expression in the same nucleus (Figs. II-8 A, B). Even 14-day and 28-day cochleotomies did not affect *occ1/Frp* mRNA expression (data not shown).

Furthermore, I examined the effect of olfactory deprivation on *occ1/Frp* mRNA expression in the mouse olfactory bulbs, in which *occ1/Frp* mRNA signals were abundantly found (Fig. II-9 B). OMP exists in maturated fibers of olfactory nerves in the glomerular layers of the olfactory bulbs (Verhaagen et al., 1990). As reported (Ducray et al., 2002), acute $ZnSO_4$ (300 mM) irrigation reduced OMP-immunoreactivity in the glomerular layer (Figs. II-9 D, G arrowheads), showing that the projection from the olfactory epithelium significantly decreased. However, *occ1/Frp* mRNA

expression was not influenced in the granular, mitral and glomerular layers in the olfactory bulbs (Figs. II-9 E, H). Significance of the density indexes of *occl/Frp* mRNA signals in the mitral cellular layer between normal and $ZnSO_4$ irrigated mice was calculated, and it was confirmed that *occl/Frp* mRNA expression was not significantly affected by olfactory deprivation ($p > 0.46$ and $p > 0.15$: control vs. 1week or 2 weeks after $ZnSO_4$ irrigation, respectively) (Figs. II-9 C, F, I, J).

These results suggest that *occl/Frp* mRNA expression is not significantly regulated by sensory activity in the mouse subcortex, and olfactory bulb unlike in macaque V1.

Discussion

In the chapter II, I compared the expression patterns of *occ1/Frp* mRNA in the neocortices of macaques, marmosets, mice, rabbits and ferrets. All specimens examined strongly expressed *occ1/Frp* mRNA in subcortical regions. In macaques and mice, subcortical patterns of *occ1/Frp* mRNA expression were similar. On the other hand, cortical patterns were markedly different among species. Similar pattern of *occ1/Frp* mRNA expression as macaque V1 was also observed in marmoset V1. *occ1/Frp* mRNA expression was, however, weak all over the mouse cortex. Strong *occ1/Frp* mRNA expression was observed in rabbits and ferrets, but was in GABAergic interneurons. Strong *occ1/Frp* mRNA expression in excitatory neurons was restricted in primates. Finally, *occ1/Frp* mRNA expression in the mouse subcortical nuclei was independent on sensory inputs. The difference in the regulation of gene transcription suggests different physiological roles of OCC1/FRP in the brains of these different species. The expression pattern of *occ1/Frp* mRNA clearly illustrates a unique primate-specific feature in the adult visual cortex at the molecular level.

1) *Subcortical expression of* occ1/Frp *mRNA in macaques and mice*

As the general understanding that the structure and function of the subcortex are relatively conserved between species than that of the neocortex, the expression pattern of *occ1/Frp* mRNA, particularly in the brainstem, was mostly conserved between macaques and mice. However, in some subcortical regions we observed several notable differences. Although reasons for such species-specific differences remain to be elucidated, the differences may become a clue to

understanding evolutional divergence as in the neocortex. For example, whereas mouse dLGB expressed *occl/Frp* in most of the cells, macaque dLGB exhibited very sparse and weak *occl* signals only in magnocellular layers (Tochitani et al. 2001). It suggests that the role of dLGB may be relegated to V1 in macaques (Hubel and Wiesel 1998). Another example is that the mouse hippocampus did not show the characteristic (CA2-specific) pattern of *occl/Frp* mRNA expression unlike macaques. The CA2-specific expression was observed also in marmosets, although *occl/Frp* mRNA was expressed strongly in all the hippocampal pyramidal cells in rabbits and ferrets (data not shown). Therefore, the CA2-specific expression of *occl/Frp* mRNA may be also a primate-specific characteristic. These phylogenetic differences in molecular property of hippocampal neurons could be correlated with the difference in the function of the hippocampus among these species (Bingman 1992, Jones 2002). Perhaps, this phylogenetic variability is related to the ability of the hippocampus to be plastic within the life of an individual, manifested, for example by the expression of immediate early genes during learning (Davis et al. 2003).

occl/Frp mRNA expression preferred glutamatergic, sensory and motor relay nuclei to cholinergic and monoaminergic nuclei in subcortical regions. Interestingly, this expression pattern overlaps that of PV in the brainstem, as well as GABAergic interneurons in the cortex. Parvizi and Damasio (2003) demonstrated that in the macaque brainstem, generally PV is abundant and CB is scarce in areas of the glutamatergic, myelinated sensory or motor pathway such as the mesencephalic trigeminal nucleus, superior olivary nucleus, ventral cochlear nucleus, facial nucleus, vestibular nuclei, and gracil nucleus. The colocalization of PV and *occl/Frp* mRNA in the brainstem and cortical GABAergic interneurons may suggest a functional involvement of OCC1 in PV-positive neurons.

2) *Brain evolution and* occ1/Frp

occ1/Frp orthologues have been identified in the mouse, rat, chick, macaque and human (Shibanuma *et al.*, 1993; Zwijsen *et al.*, 1994; Patel *et al.*, 1996; Tochitani *et al.*, 2001). Taking the macaque as a standard, the homologies of the nucleotide sequences of the coding regions in these species are high (99%, 89%, 89% and 78% for the human, mouse, rat and chick, respectively), suggesting conserved function among species. However, the transcriptional regulation of *occ1/Frp* in the cerebral cortices obviously differs. While unique interareal and interspecies differences have been reported for the distribution patterns of Ca^{2+}-binding proteins (PV, CB and CR) and non-phosphorylated neurofilaments (DeFelipe, 1993; Glezer *et al.*, 1993; Hof *et al.*, 2000), the difference in *occ1/Frp* mRNA expression was more notable even within euarchontoglires (Murphy *et al.*, 2001). Furthermore, it should be noted that the most characteristic *occ1/Frp* mRNA expression pattern was observed in primate V1, one of the most evolutionarily distinct cortical areas (see for example Nieuwenhuys, 1994).

I discussed in chapter I about the genetic contribution to *occ1* mRNA expression, as well as neuronal activity. It appears that the genetic program of the activity-dependent expression of *occ1/Frp* mRNA is acquired only in the primate lineage, since in other species, regions that exhibit a high CO activity, such as the rodent barrel field (Wong-Riley and Welt, 1980), did not show a strong *occ1/Frp* mRNA expression, and *occ1/Frp* mRNA expression in excitatory neurons in the mouse dLGN, the anteroventral cochlear nucleus and the olfactory bulb was independent of sensory deprivation.

Recent studies have suggested that nonsynonymous nucleotide substitutions with significant amino acid substitutions are associated with the evolution of the human brain (Clark *et al.*, 2003; Dorus *et al.*, 2004). On the other hand, microarray studies also suggested that changes in the

temporal and spatial patterns of gene expression are important in brain evolution (Cáceres *et al.*, 2003; Preuss *et al.*, 2004). I consider that *occ1/Frp* is a typical example of modifications of transcriptional regulation in a cell-type specific and activity-dependent manner without significant changes in the coding sequence. I believe that the exploration of evolutional changes on physiological role and transcriptional regulation of *occ1* will shed the light to understanding the evolution of the primate neocortex.

Figures and Table

Figure II-1

Sagittal sections for ISH of occ1/Frp of marmoset (A), mouse (B), rabbit (C) and ferret (D). Upper is dorsal and right is rostral. Arrows indicate V1/V2 borders in marmoset neocortex. Scale bar = 9 mm for A, C, E and 3 mm for B.

Figure II-2

A-C: Coronal section for ISH of *occ1* (B), and adjacent Nissl-stained (A) and CO-stained sections (C) of marmoset visual cortex. Upper is dorsal and right is medial. Arrows indicate V1/V2 borders. Scale bar in A = 1.0 mm. ca/calcarine sulcus. D-I: Coronal sections for ISH of *occ1* antisense (E, H) and sense probes (F, I), and adjacent Nissl-stained sections (D, G) of marmoset primary visual (D-F) and motor (G-I) cortices. Scale bar in D = 300 μm.

Figure II-3

Coronal sections for ISH of *occ1/Frp* (B, D, F, H, J), and adjacent Nissl-stained sections (A, C, E, G, I) of mouse visual (A, B), mouse somatosensory (C, D), rabbit visual (E, F), ferret frontal (G, H) or ferret visual cortices (I, J). Arrowheads in A and B indicate V1/V2 borders and the arrow in C

indicates the barrel field (BF) in layer IV of the mouse primary somatosensory cortex. Scale bar in A = 300 μm for all sections.

Figure II-4

Coronal sections of ferret (A, B) and rabbit (C, D) visual cortex for double ISH of *occ1/Frp* (red) and either PV (A, C) or CB (B, D) (green). Scale bar = 150 μm.

Figure II-5

Various subcortical sections for ISH of *occ1* (left panels) and adjacent Nissl-stained sections (right panels) in macaques. Left is medial and upper is dorsal. Scale bar in A = 1 mm for A-K, and 77 μm for L. For abbreviations, refer to Table 2.

Figure II-6

Various subcortical sections for ISH of *occ1/Frp* (left panels) and adjacent Nissl-stained sections (right panels) in mice. Left is medial and upper is dorsal. Scale bar in A = 840 μm for A, 500 μm for B-K and 50 μm for L. For abbreviations, refer to Table 2.

Figure II-7

Coronal sections for ISH of *occ1/Frp* (A, B, E, F) and adjacent CO-stained sections (C, D, G, H) of normal mouse dLGN (A, C), binocularly enucleated (survival time was 14 days) (B, D) and monocularly enucleated (survival time was 14 days) adult mouse dLGN (E-H). E and G are ipsilateral, and F and H are contralateral to the enucleated eye. Note that CO activity decreased in the dLGN of binocularly deprived mouse (D), in the binocular region (Bi) ipsilateral to the enucleated eye (G), and in both the monocular region (Mo) and binocular regions contralateral to the enucleated eye (H) in the dLGN of monocularly deprived mouse, whereas there were no significant changes in *occ1/Frp* mRNA expression in the same dLGNs (B, E, F). Scale bar in A = 300 μm. Upper is dorsal. Left is lateral in A-G, and right is lateral in F and H.

Figure II-8

Coronal sections for ISH of *occ1/Frp* (A, B) and adjacent sections stained for GAP43-immunoreactivity (C, D) in the anteroventral cochlear nucleus (AVCN) of a unilateral auditory deprived (the survival time was 7 days) adult mouse. A and C are contralateral, and B and D are ipsilateral to site of cochleotomy. Note that GAP43 immunoreactivity was enhanced in the case of ipsilateral cochleotomy (D, arrowheads), whereas no significant changes in *occ1/Frp* expression level in the same nucleus (C). Scale bar = 300 μm.

Figure II-9

Coronal sections for ISH of *occl/Frp* (B, E, H) and adjacent sections stained for OMP-immunoreactivity (A, D, G) in the olfactory bulb of normal (A, B) and olfactory deprived adult mice (D, E, G, H). The survival time was 7 days (D, E) or 14 days (G, H). Note that OMP-immunoreactivity decreased in the case of olfactory deprivation (D, G, arrowheads), showing that the projection from the olfactory epithelium significantly decreased by intranasal $ZnSO_4$ irrigation, whereas no significant changes in *occl/Frp* expression level in the same olfactory bulbs (E, H). Scale bar = 500 μm. C, F, I show density indexes of *occl/Frp* mRNA signals in the square regions in B, E, H, respectively. J is the statistics of density indexes in the mitral cellular layers. The figures in the parentheses indicate the number of mice examined. No significant changes of density indexes of occl/Frp signals by olfactory deprivation were observed ($p>0.46$ for control vs. survival time 1 week after ZnSO4 irrigation, and $p>0.15$ for control vs. survival time 2 weeks). Gr/granule cellular layer, M/mitral cellular layer, Gl/glomerular layer

Table II-1

Signal intensities of *occl/Frp* mRNA in macaque and mouse subcortices. The intensities were estimated into four grades (-, ±, + and ++). Representation by more than two grades (e.g., - ~ +) means a variation of signal intensities within the nucleus. Nuclei that are not listed here exhibited only faint or no signals (± or -) both in macaques and mice. The grades of difference between two species are represented by ☆☆, ☆, ★ and ★★, more different in this order. nd/not determined s/scattered

Figure II-1

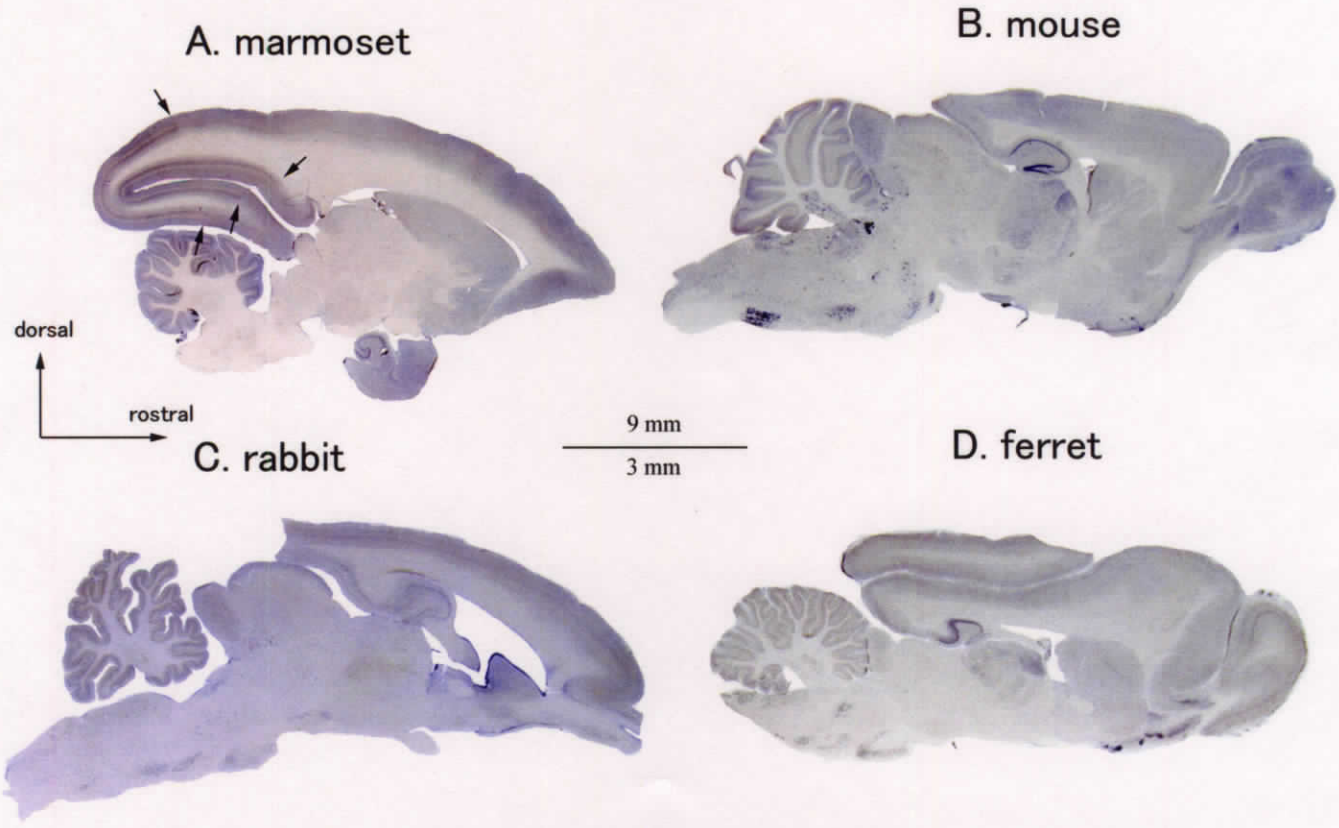

Figure II-2

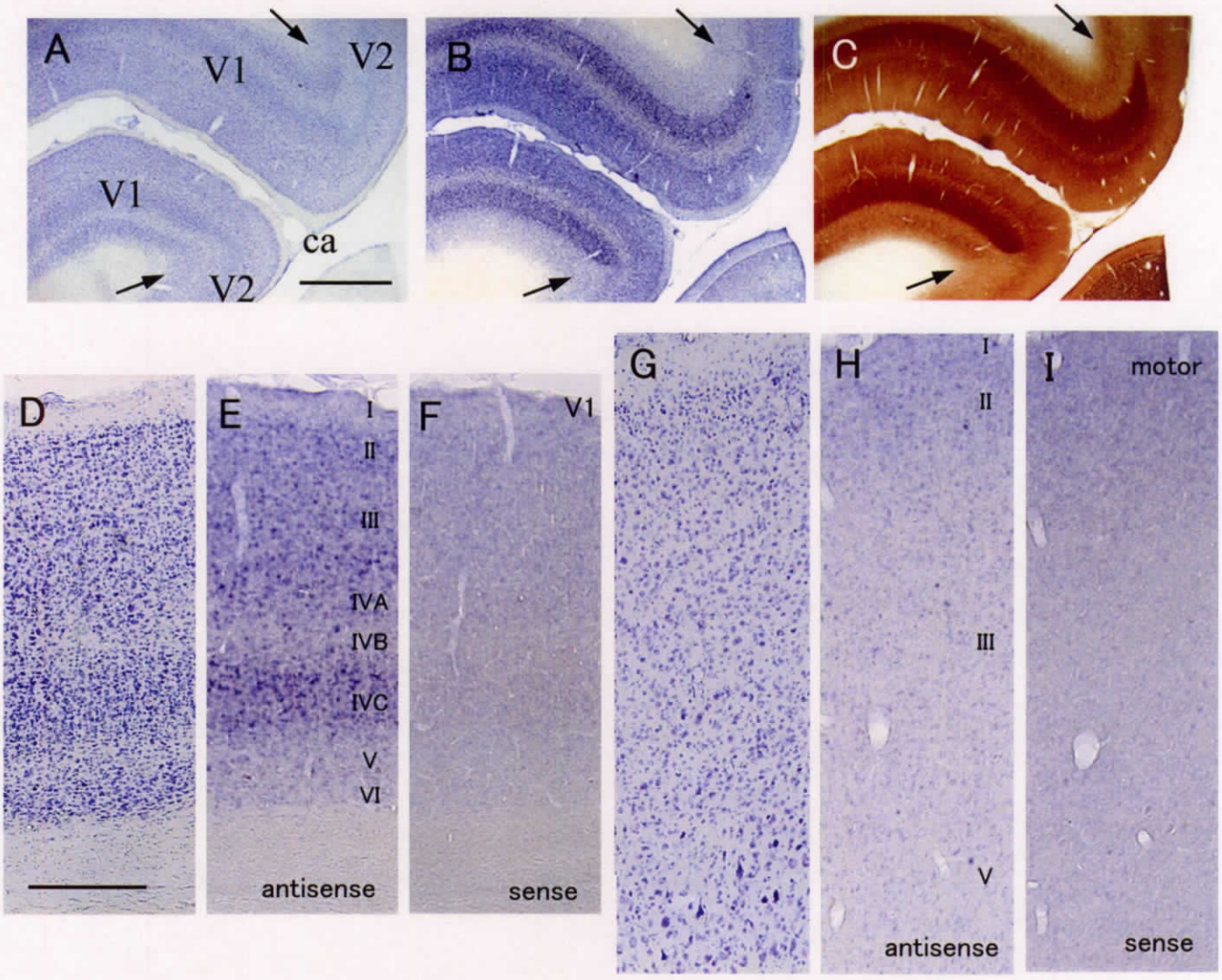
A
V1
V2
V1
ca
V2
B
C
D
E
I
II
III
IVA
IVB
IVC
V
VI
antisense
F
V1
sense
G
H
I
II
III
V
antisense
I
motor
sense

Figure II-3

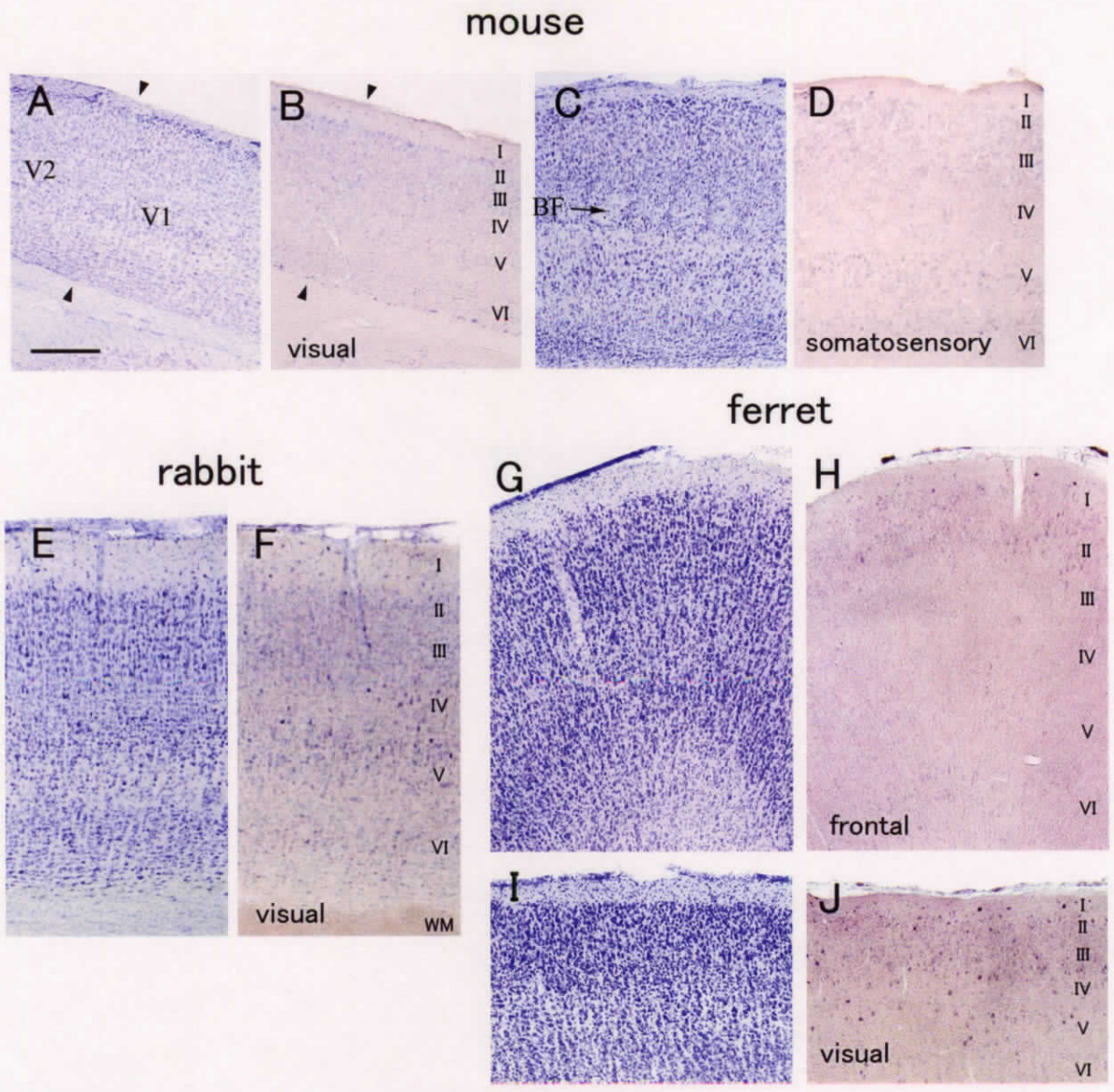
mouse
A
V2
V1
B
I
II
III
IV
V
VI
visual
C
BF
D
somatosensory
rabbit
E
F
visual
WM
ferret
G
H
frontal
I
J
visual

Figure II-4

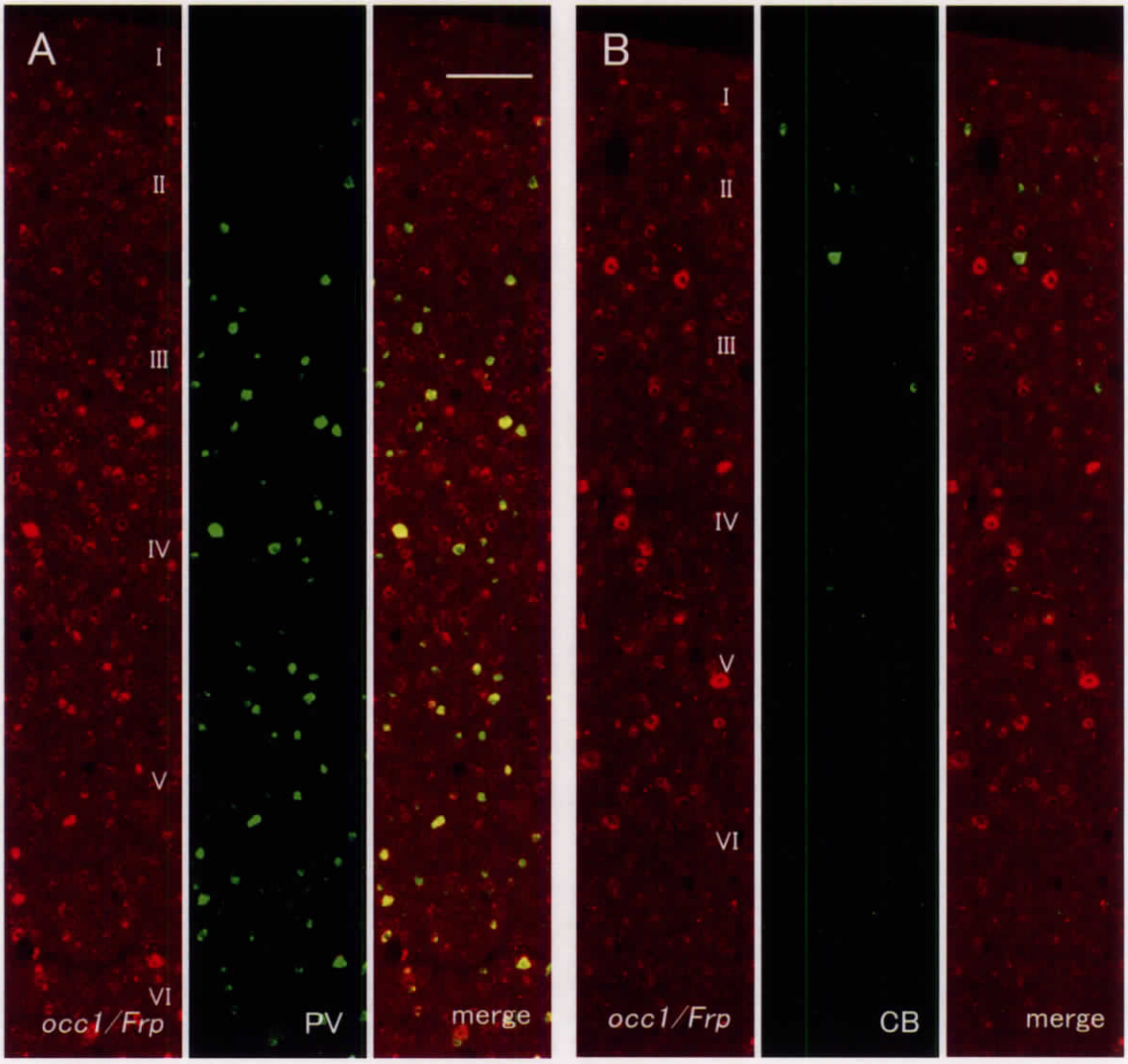
A
I
II
III
IV
V
VI
occ1/Frp
PV
merge
B
I
II
III
IV
V
VI
occ1/Frp
CB
merge

Figure II-4 continuation 1

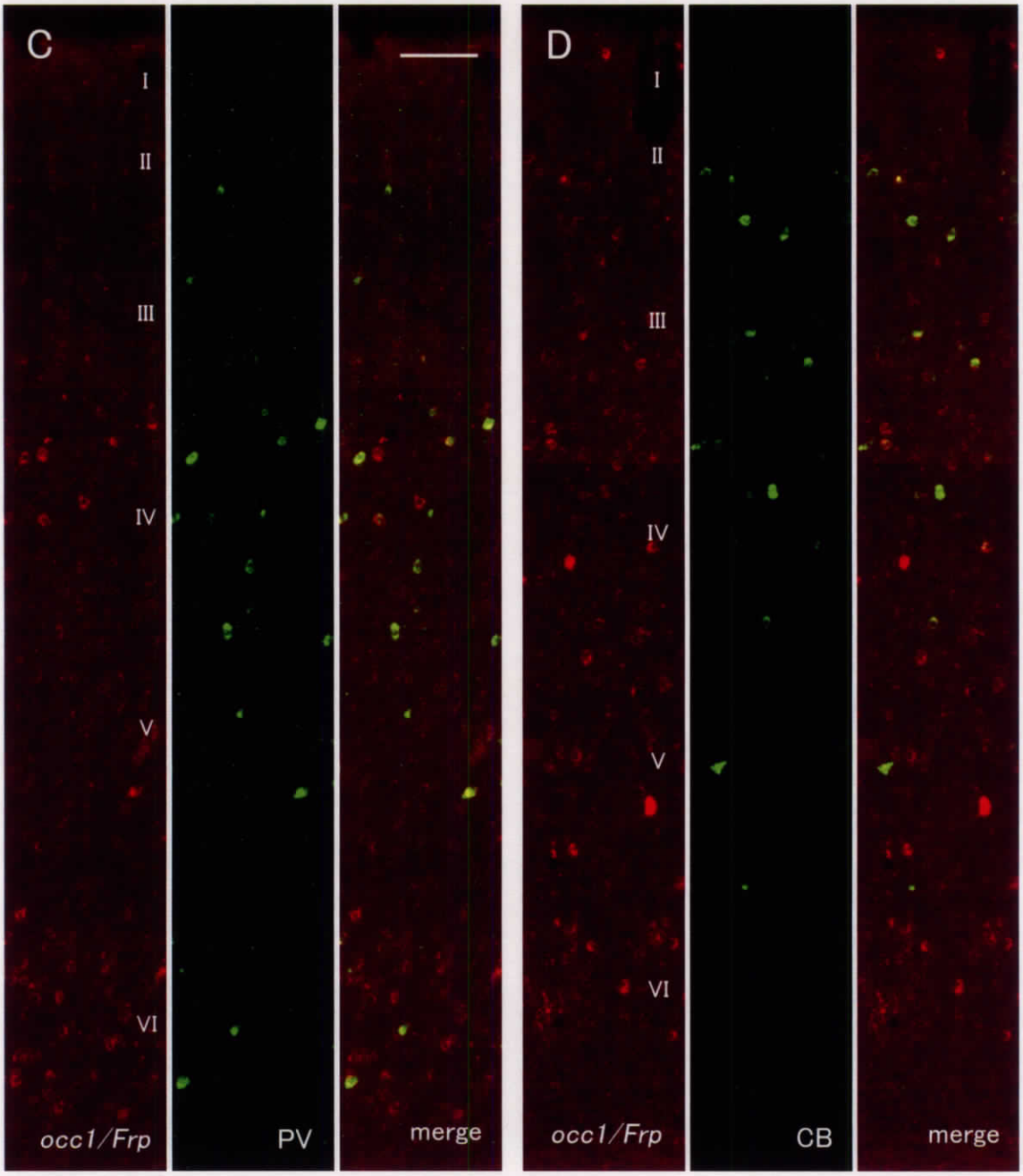

Figure II-5

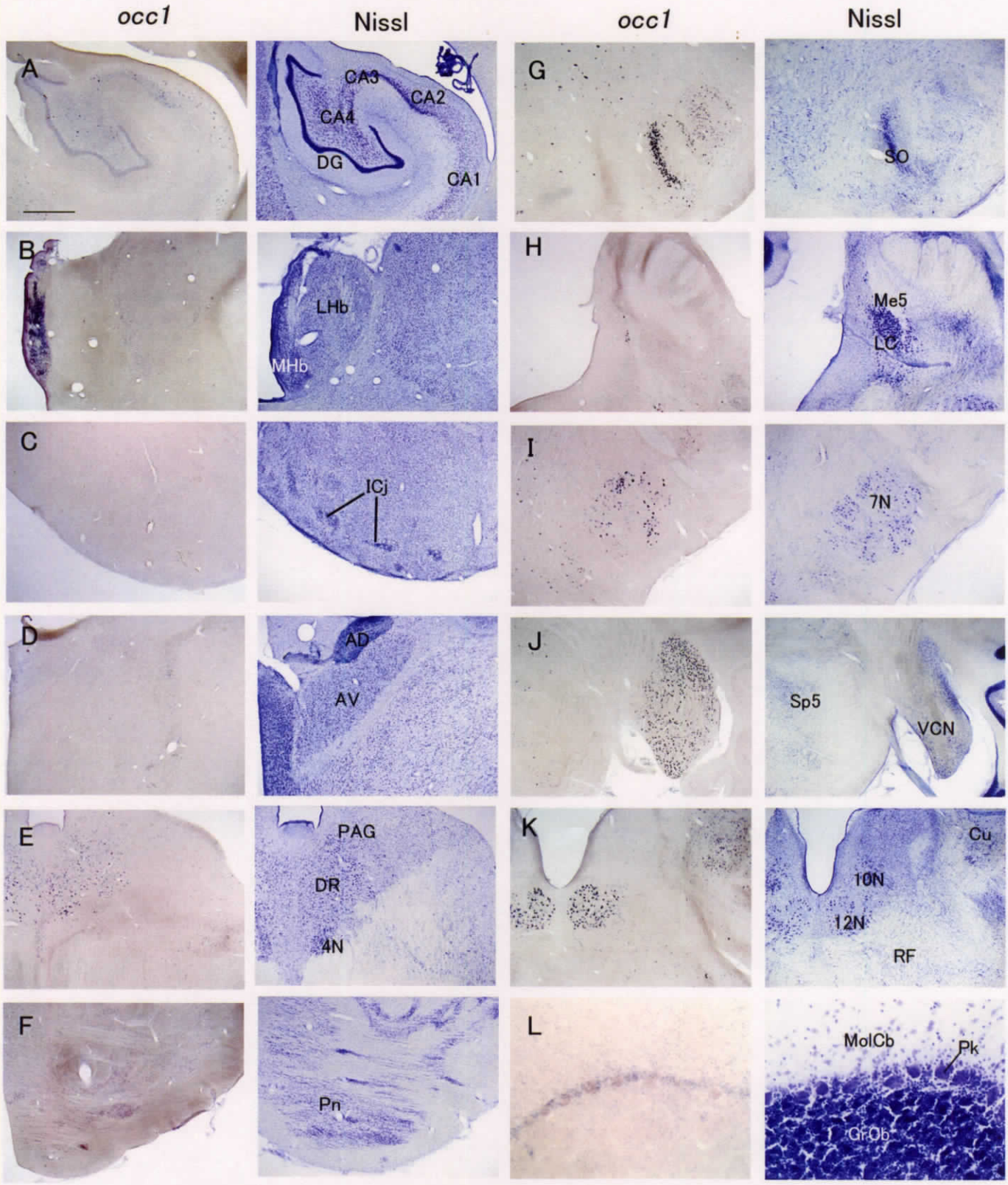
occ1
Nissl
occ1
Nissl
A
CA3
CA2
CA4
DG
CA1
G
SO
B
LHb
MHb
H
Me5
LC
C
ICj
I
7N
D
AD
AV
J
Sp5
VCN
E
PAG
DR
4N
K
Cu
10N
12N
RF
F
Pn
L
MolCb
Pk
GrOb

Figure II-6

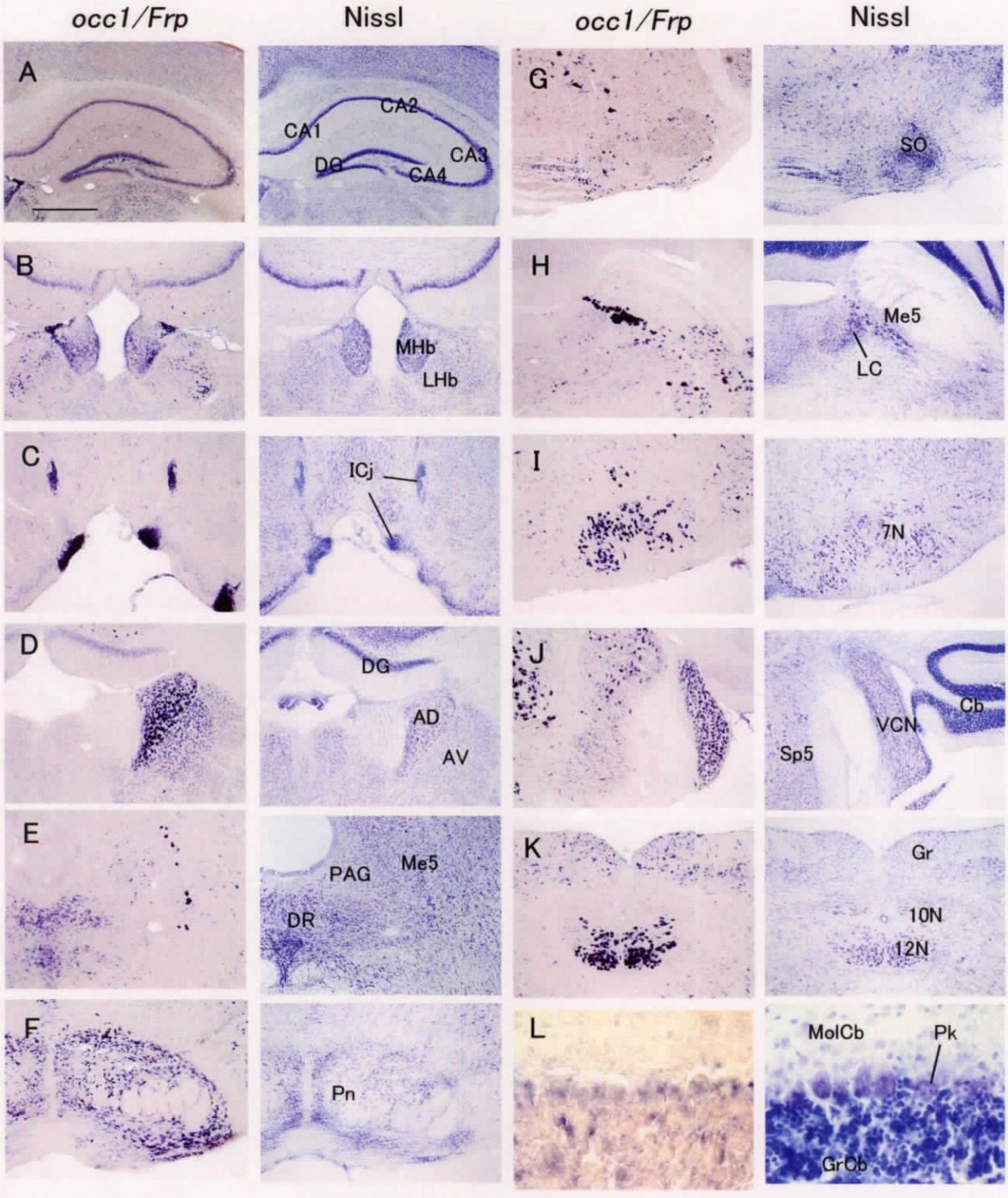
occ1/Frp
Nissl
occ1/Frp
Nissl
A
CA1
CA2
CA3
DG
CA4
G
SO
B
MHb
LHb
H
Me5
LC
C
ICj
I
7N
D
DG
AD
AV
J
Cb
VCN
Sp5
E
PAG
Me5
DR
K
Gr
10N
12N
F
Pn
L
MolCb
Pk
GrCb

Figure II-7

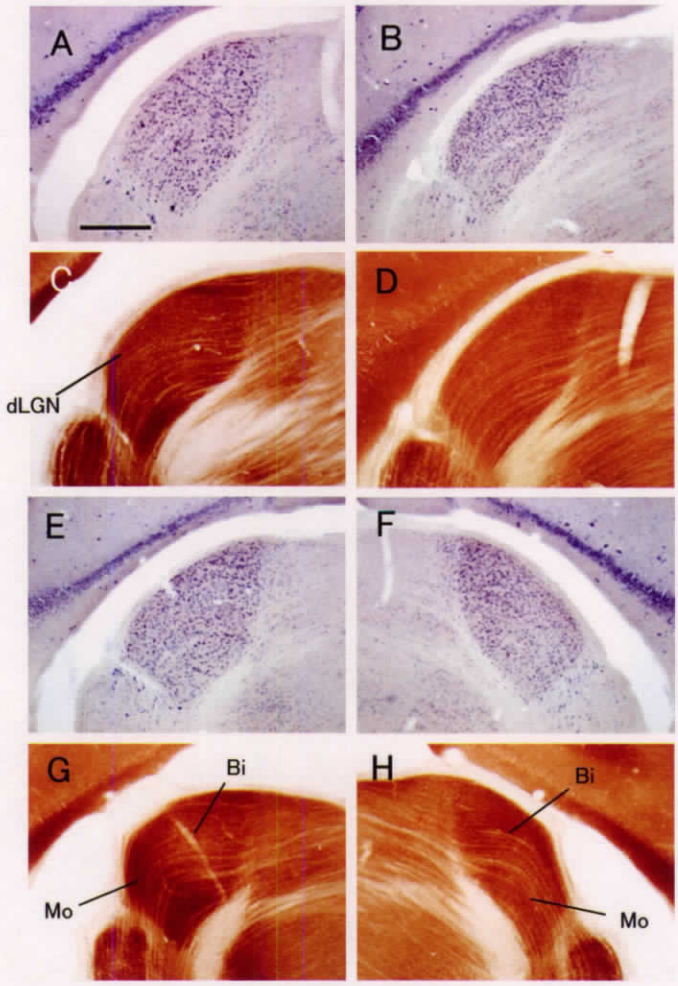

Figure II-8

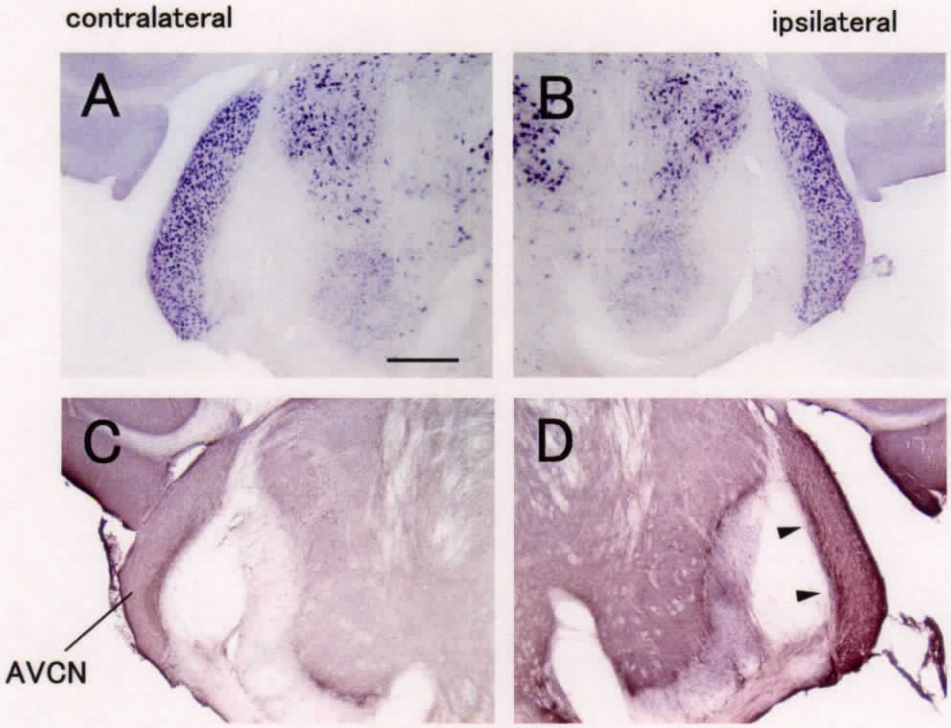

Figure II-9

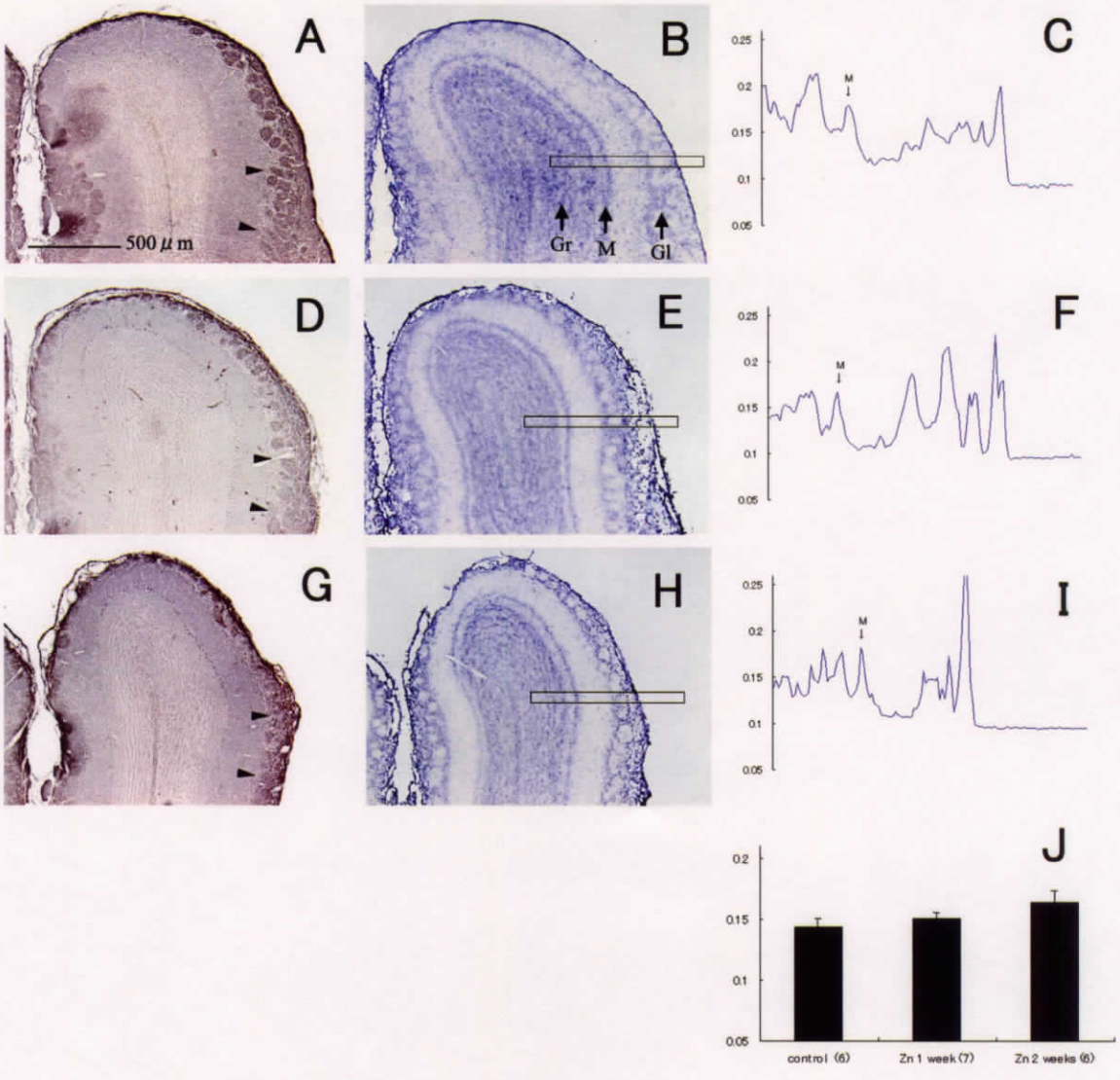
A
500 μ m
B
Gr
M
Gl
C
M
0.25
0.2
0.15
0.1
0.05
D
E
F
M
0.25
0.2
0.15
0.1
0.05
G
H
I
M
0.25
0.2
0.15
0.1
0.05
J
0.2
0.15
0.1
0.05
control (6)
Zn 1 week (7)
Zn 2 weeks (6)

Table II-1

		macaque	mouse	
olfactory bulb	mitral cell layer (Mi)	nd	±	
	granule cell layer (GrO)	nd	±	
	glomerular layer (Gl)	nd	±	
	anterior olfactory nucleus (AOL)	-	+	★
basal ganglia	caudate nucleus (Cd) (caudate putamen : CPu)*	- ～ + (s)	- ～ ± (s)	☆
	putamen (Pu)	- ～ + (s)		☆
	amygdaloid body (Amy)	- ～ + (s)	±	☆
septo-hippocampal area	lateral septal nucleus (LS)	±	+	☆
	septofimbrial nucleus (Sfi)	±	±	☆☆
	islands of Calleja (ICj)	-	++	★★
	pyramidal layer of CA1, 3 and 4	-	+	★
	pyramidal layer of CA2	+	+	☆☆
	granule cell layer of dentate gyrus (GrDG)	±	+	☆
	subiculum (S)	± ～ +	++	★
	interneurons in hippocampul formation	- ～ + (s)	- ～ + (s)	☆☆
diencephalon	medial habenular nucleus (MHb)	++	+ ～ ++	☆
	lateral habenular nucleus (LHb)	-	- ～ +	☆
	anterior thalamic nuclei (Ath)	- ～ ±	++	★★
	medial thalamic nuclei (Mth)	- ～ ±	±	☆
	ventolateral thalamic nuclei (VLth)	- ～ ±	± ～ +	☆
	reticular thalamic nucleus (Rt)	±	±	☆☆
	zona incerta (ZI)	- ～ ±	± ～ +	☆
	dorsal lateral geniculate body (dLGB)	- ～ ± (s)	+	★
	medial geniculate body (MGB)	-	±	☆
	supraoptic nucleus (SOp)	+	±	☆
	hypothalamic nuclei (Hy)	± ～ +	± ～ +	☆☆
	subthalamic nucleus (STh)	+	+	☆☆
	median eminence (ME)	nd	+	
	lateral mammillary nucleus (LM)	±	+	☆
brain stem	mesencephalic reticular formation (MeRt)	±	- ～ +	☆
	Darkshewitsch nucleus (Dk)	-	±	☆
	interstitial nucleus of Cajal (InC)	±	±	☆☆
	red nucleus, magnocellular part (RMC)	-	+	★
	red nucleus, parvicellular part (RPC)	-	- ～ +	☆
	interpeduncular nucleus (IP)	±	- ～ ±	☆
	substantia nigra (SN)	± ～ +	- ～ ±	☆
	supirior colliculus (SC)	±	±	☆☆
	inferior colliculus (IC)	±	±	☆☆
	oculomotor nucleus (3N)	+	++	☆
	trochlear nucleus (4N)	-	+	★
	mesencephalic trigeminal nucleus (Me5)	++	++	☆☆
	locus coeruleus (LC)	-	-	☆☆
	pontine nuclei (Pn)	±	++	★
	periaquoductal gray (PAG)	- ～ ±	±	☆
	dorsal raphe nucleus (DR)	± ～ +	± ～ +	☆☆
	median raphe nucleus (MR)	- ～ +	± ～ +	☆
	pontine and medullary reticular formation (RF)	± ～ +	± ～ +	☆☆
	reticulotegmental nucleus (RtTg)	+	++	☆
	dorsal nucleus of lateral lemniscus (DLL)	±	±	☆☆
	periolivary region (PO)	± ～ +	+	☆
	motor trigeminal nucleus (Mo5)	++	++	☆☆
	principal trigeminal nucleus (Pr5)	+	++	☆
	ventral tegmental nucleus (VTg)	±	++	★
	parabranchial nucleus (PB)	-	- ～ ±	☆
	trapezoid body (tz)	±	±	☆☆
	supirior olivary nucleus (SO)	++	±	★
	dorsal tegmental nucleus (DTg)	+	- ～ ±	★
	pontine raphe nucleus (PnR)	- ～ +	±	☆
	abducens nucleus (6N)	± - +	+	☆
	facial nucleus (7N)	++	++	☆☆
	vestibular nuclei (Ve)	± ～ +	± ～ +	☆☆
	prepositus nucleus (Pr)	±	+ ～ ++	★
	ventral cochlear nucleus (VCN)	++	++	☆☆
	dorsal cochlear nucleus (DCN)	+	±	☆
	spinal trigeminal nucleus (Sp5)	±	± ～ +	☆
	dorsal motor nucleus of vagus (10N)	-	- ～ ±	☆
	hypoglossal nucleus (12N)	++	++	☆☆
	inferior olivary nucleus (IO)	-	±	☆
	lateral reticular nucleus (LRt)	± ～ +	++	★
	ambiguus nucleus (Amb)	- ～ +	++	★
	external cuneate nucleus (ECu)	++	++	☆☆
	cuneate nucleus (Cu)	+	+	☆☆
	gracil nucleus (Gr)	+	+	☆☆
cerebellum	cerebellar nuclei (Cbn)	±	++	★
	granule cell layer (GrCb)	- ～ ± (s)	- ～ ± (s)	☆☆
	Purkinje cells (Pk)	-	-	☆☆
	Bergman glias (Bg)	±	±	☆☆

Materials and Methods

1) *Tissue preparation*

Eight macaques (*Macaca fuscata*, adult, either sex, 2.9-4.7 kg), three common marmosets (*Callithrix jacchus*, adult, either sex, 300-500 g), fifty mice (*Mus musculus*, forty-four ICR and six C57BL/6 (SLC Japan), 10-13 weeks old, either sex, 20-40 g), two rabbits (*Oryctolagus cuniculus*, adult, either sex, 2.8-3.8 kg) and five ferrets (*Mustela putorius*, adult, male, 1.1-1.5 kg) were used in this study. In four of the eight macaques, tetrodotoxin (TTX; 15 μg in 10 μl of normal saline) was injected repeatedly (twice a week) under ketamine anesthesia into the vitreous cavity of the left eye and the macaques were kept alive for 7, 10 or 14 days. These monocularly deprived macaque cortices were used also in our previous study (Tochitani *et al.*, 2001). The eye enucleation surgery on mice was conducted under deep anesthesia (Nembutal 30-50 mg/kg body weight) as follows (Nie and Wong-Riley, 1996). Ten mice were enucleated on one side (left), and three mice were enucleated on both sides at 10-12 weeks old. Then the eyelid of the enucleated side was sutured and treated with ointment and antibiotic, and the mice were kept alive for 7 or 14 days. I used four C57BL/6 mice for the monocular deprivation experiment and one for the binocular deprivation experiment, considering that the retina of albino mice may be injured spontaneously and the neuronal activity in the visual pathways of the ICR strain is considerably low (Serfilippi *et al.*, 2004). However, since I could confirm essentially the same results from both strains, results obtained from both strains were used equally in the following description. Thirteen mice were unilaterally cochleotomized under deep anesthesia (Nembutal 30-50 mg/kg body weight) as follows (Illing, 2001). Approached through behind the right auricle, I removed the eardrum and the middle ear bones, penetrated the cochlea

with a needle, and aspirated lymph inside of the cochlea. After treatment of ointment and antibiotic, I sutured the wound. Postoperative survival time was 7, 14, or 28 days. Olfactory deprivation was performed on twelve ICR mice by intranasal irrigation of $ZnSO_4$ (Ducray et al., 2002). Under light ether anesthesia, 0.3-0.5 ml of ZnSO4 (300 mM) in PB was repeatedly (2-4 times) injected into both nasal cavities with blunt end-needles, and survival time was 7 or 14 days. All animals were administered an overdose of Nembutal (at least 100 mg/kg body weight) and perfused intracardially with 4% paraformaldehyde (PFA) in 0.1M phosphate buffer (PB, pH 7.4). The brain was then removed from the skull, postfixed for 3-6 h at 4℃ (mice, rabbits and ferrets) or room temperature (marmosets and macaques) in the same fixative, cut into several blocks and cryoprotected in 30% sucrose in 0.1 M PB at 4℃. The blocks were cut as frozen sections on a sliding microtome at 15-40 μm thick. The sections were maintained in a cryoprotectant solution (30% glycerol, 30% ethylene glycol and 40% 0.1 M phosphate-buffered saline (PBS), pH 7.4) at -30℃ when they were not used for more than 24 h after sectioning until experiment. Frozen block samples were stored at -30℃.

The protocols of the present study were approved by the Animal Research Committee of the National Institute for Basic Biology and the National Institute for Physiological Science, Japan, and followed the animal care guidelines of NIH, USA.

2) *Histological analysis*

For colorimetric ISH, digoxigenin (DIG)-labeled antisense and sense riboprobes were prepared using a DIG-dUTP labeling kit (Roche Diagnostics, Indianapolis, IN). Probes and primers used for this study are listed in Table M-1. For marmosets, mice, rabbits and ferrets, more than two types of probe for *occl/Frp* were prepared. Since each probe exhibited essentially the same patterns of signal

distribution when used separately (data not shown), we mixed the probes to enhance signals. Sense probes detected no signals higher than the background signal. ISH was carried out as described previously (Tochitani *et al.*, 2001). Briefly, free-floating sections (35-40 μm thick) were soaked in 4% PFA in 0.1M PB (pH 7.4) overnight at 4℃ and treated with 1-10 μg/ml proteinase K for 30 min at 37℃. After acetylation, the sections were incubated in hybridization buffer (5×SSC, 10% blocking reagent, 50% formamide, 0.1% N-lauroylsarcosine (NLS), 0.1% SDS) containing 1.0 μg/ml DIG-labeled riboprobe at 60-65 ℃ overnight. Hybridized sections were washed by successively immersing in washing buffer (2×SSC, 50% formamide, 0.1% NLS; 60-65℃, 20 min, twice), RNase A buffer (10 mM Tris-HCl, 10 mM EDTA, 0.5 M NaCl, pH 8.0) containing 20 μg/ml RNase A (37℃, 15 min), 2×SSC/0.1% NLS (37℃, 20 min, twice) and 0.2×SSC/0.1% NLS (37℃, 15 min, twice). Hybridization signals were visualized by alkaline phosphatase (AP) immunohistochemical staining using a DIG detection kit (Roche Diagnostics). After mounting onto glass slides, the sections were dehydrated through a graded series of increasing ethanol concentration followed by xylene, and then coverslipped with Entellan new (Merck, Tokyo, Japan). The ISH signals in marmoset samples were generally weak, and the signal/noise ratio was not as high as that for the other mammalian samples and double ISH data were unavailable.

Fluorescence double ISH was performed as described previously (Komatsu *et al.*, 2005). Fluorescein (FITC)-labeled riboprobes for γ-amino butyric acid (GABA)-ergic marker genes (glutamic acid decarboxylase 67 (GAD67), parvalbumin (PV), calbindin D-28k (CB) and calretinin (CR)) and a glutamatergic marker, vesicular glutamate transporter 1 (VGLUT1) were prepared (see supplementary Table, for probes used). Brain sections (15 μm thick) were hybridized with the DIG-labeled *occl/Frp* probe and either the FITC-labeled GABAergic probe or the glutamatergic marker probe. The hybridization protocol was the same as that of colorimetric single ISH. DIG was detected by staining with AP-conjugated anti-DIG antibodies and using a HNPP Fluorescence

Detection kit (Roche Diagnostics). FITC was detected by staining with horseradish peroxidase-conjugated anti-FITC antibodies (Roche Diagnostics) followed by enhancement using a TSA-Plus DNP system (PerkinElmer Life Sciences, Boston, MA) and staining with alexa 488-conjugated anti-DNP antibodies (Molecular Probes, Eugene, OR). After mounting onto glass slides, sections were air-dried and then coverslipped with the PermaFluor Aqueous mounting medium (Thermo, Pittsburgh, PA).

To visualize cytochrome oxidase (CO) activity, sections were immersed in 0.33 mg/ml cytochrome C type III (Sigma, Tokyo, Japan), 0.54 mg/ml 3'3-diaminobenzidine (DAB), and 4.5% sucrose in 0.1M PB (pH 7.4) and incubated in the dark at 37℃ for 4-5 h (Wong-Riley, 1979). For Nissl staining, sections were mounted onto glass slides, air-dried and stained with thionine. In both procedures, the sections were dehydrated through a graded series of increasing ethanol concentration followed by xylene and coverslipped with Entellan new.

Immunohistochemistry was performed to visualize immunoreactivity of growth-associated protein 43 (GAP43) and olfactory marker protein (OMP) as follows. After blocking in the blocking buffer (0.5% Triton X-100, 5% skimmmilk in PBS, room temperature, 1 h), sections were soaked into the reaction buffer (0.5% Triton X-100, 1% skimmmilk in PBS) containing the primary antibodies (4℃, overnight). Anti-GAP43 mouse monoclonal antibody was commercially available (clone GAP-7B10, Sigma), and anti-OMP goat antiserum was kindly gifted by Dr. Margolis. Sections were then washed in PBS three times and reacted by the secondary antibodies conjugated by biotin (room temperature, 2 h). Finally, immunoreactivity was detected using avidin/biotin/HRP detection kit (Vectastain, CA) with Nickel enhancement. The sections were dehydrated through a graded series of increasing ethanol concentration followed by xylene and coverslipped with Entellan new.

The cortical areas in macaques and mice were identified using brain atlases (Paxinos *et al.*, 2000; Paxinos and Franklin, 2001) and by comparing adjacent Nissl-stained sections. The cortical areas of

marmosets, rabbits and ferrets were determined by Nissl staining, parvalbumin immunostaining and CO staining of adjacent sections. The scale bars in figures are corrected for shrinkage caused by ISH.

3) *Statistical analysis*

To quantify double ISH data, I counted the number of cells exhibiting signals. The data for each animal were represented by one or two bins (690 μm width) from layers I to VI in vertical sections. The areas in which cells were counted were calculated, and cell numbers were normalized to per mm^2. Signals were magnified 20 times under a darkfield microscope and counted manually. Signals not arising from neurons were excluded from the calculation. To estimate objectively, another researcher counted the numbers of signals separately. Since the count error was sufficiently small (the errors between the two counters were 12.9 ± 2.7, 5.5 ± 1.4 and 5.2 ± 0.8 for the number of GABAergic markers, number of double-positive cells, and ratios, respectively), results obtained by me were used in this paper. The significance of differences between results from the nondeprived column and those from the deprived column in the experiment of monocular deprivation of macaque V1 was analyzed by paired Student's *t*-test.

Density indexes of *occl/Frp* mRNA signals were calculated in 58 μm (vertical) × 808 μm (horizontal) squares in the mouse olfactory bulbs to quantify the degree of the effect of olfactory deprivation on *occl/Frp* mRNA expression, using an image analyzer (Image pro plus) (Fig. II-9). The peak values in mitral cellular layers were compared between normal and $ZnSO_4$ treated mice, and the significance was analyzed by unpaired Student's *t*-test.

Table M-1

Probes used in the present study. Two or three types of *occl/Frp* probe were prepared for mice, rabbits, ferrets and marmosets. Degenerate primers were used to clone cDNAs for different species. *: used in a previous study by Tochitani et al. (2001). **: used in a previous study by Komatsu et al. (2005). ***: The same probe as for macaque GAD67 was used for ferret and rabbit GAD67. ****: The same probes as for ferret PV, CB and CR were used for rabbit PV, CB and CR, respectively.

Table M-1

	Subject	cDNA from	Accession No.	Forward Primer	Reverse Primer	Position
occ1/Frp	macaque*	macaque	AB039661 (macaque)	5'-ggatccaaaatccaggttga-3'	5'-agatctctttggtgctcact-3'	333-999
	marmoset 1	marmoset	AB039661 (macaque)	gccaatgtgttytgyggngc	ttgatggcwgtytcrttytg	168-613
	marmoset 2	marmoset	AB039661 (macaque)	gcagatcaggaraayaayaa	ttcttggtcttytcngcngt	627-979
	mouse 1	mouse	XM_147260 (mouse)	aagatccaggttgattatga	catatcctgtcttctcctcc	338-932
	mouse 2	mouse	XM_147260 (mouse)	gggcacagcagaaaagaccaag	ttgggaccaaaaggagaagcag	955-1471
	mouse 3	mouse	XM_147260 (mouse)	gtgaaggggtttgggcatttt	aggcacttggagaggggatga	1801-2769
	rabbit 1	rabbit		same as marmoset 1		
	rabbit 2	rabbit		same as marmoset 2		
	ferret 1	ferret		same as marmoset 1		
	ferret 2	ferret		same as marmoset 2		
VGLUT1	macaque**	macaque	AB032436 (human)	ccgctacattatcgccatca	cgatgggcacgatgatggtc	204-1093
GAD67	macaque**	macaque	BC037780 (human)	gagctgatggcgtcttcgac	cgttgatgtcagccattctc	417-1046
	(ferret, rabbit)***					
PV	macaque	macaque	NM_002854 (human)	gcaggatgtcgatgacagac	tttcagccaccagagtggag	52-384
	ferret (rabbit)****	ferret	NM_002854 (human)	gcaggatgtcgatgacngay	cagccaccagagtngaraay	52-381
CB	macaque	macaque	NM_004929 (human)	acgctgacggaagtggttac	tgtactgactggcctaagcat	253-1200
	ferret (rabbit)****	ferret	NM_004929 (human)	cacagtttttcgarathtgg	cggtacagcttnccnccrtc	223-928
CR	macaque	macaque	NM_007088 (human)	ctggaaatctgggarcaytt	tcactgcagagnacdatytc	134-873
	ferret (rabbit)****	ferret		same as macaque CR		

Acknowledgement

This thesis was supported by many people.

I greatly thank Prof. Yamamori in the National Institute for Basic Biology (NIBB) for providing the chance and environment to investigate exciting research material about *occl*. I thank Drs. Watakabe and Komatsu and other members of the Division of Brain Biology in NIBB for their wisdom and technical supports. I am appreciative of the helpful advices and technical contribution from Dr. Hashikawa in Brain Science Institute at RIKEN. Prof. Sakano and Dr. Tsuboi in University of Tokyo supported the olfactory deprivation experiment. Dr. Margolis in University of Maryland kindly gifted anti-OMP antiserum. Drs. Rockland and Tochitani in RIKEN provided me valuable suggestions for writing the paper. Daiko Foundation in Nagoya financially supported me. And I greatly appreciate my parents, grandmother and brother for their financial and mental supports all through my life.

Finally, I am grateful and pray for the sacrifice of many experimental animals.

References

Benson DL, Isackson PJ, Gall CM, Jones EG (1991) Differential effects of monocular deprivation on glutamic acid decarboxylase and type II calcium-calmodulin-dependent protein kinase gene expression in the adult monkey visual cortex. J Neurosci 11:31-47.

Bingman VP (1992) The importance of comparative studies and ecological validity for understanding hippocampal structure and cognitive function. Hippocampus 2:213-219.

Blumcke I, Weruaga E, Kasas S, Hendrickson AE, Celio MR (1994) Discrete reduction patterns of parvalbumin and calbindin D-28k immunoreactivity in the dorsal lateral geniculate nucleus and the striate cortex of adult macaque monkeys after monocular enucleation. Vis Neurosci 11:1-11.

Brekken RA, Puolakkainen P, Graves DC, Workman G, Lubkin SR, Sage EH (2003) Enhanced growth of tumors in SPARC null mice is associated with changes in the ECM. J Clin Invest 111:487-495.

Brodmann L (1909) Vergleichende localisationslehre der grosshirnrinde in ihren prinzipien dargestellt auf grund des zel lenbaues. Leipzig: Barth.

Caceres M, Lachuer J, Zapala MA, Redmond JC, Kudo L, Geschwind DH, Lockhart DJ, Preuss TM, Barlow C (2003) Elevated gene expression levels distinguish human from non-human primate brains. Proc Natl Acad Sci U S A 100:13030-13035.

Casagrande VA, Kaas JH (1994) The afferent, intrinsic, and efferent connections of primary visual cortex in primates. In: Cerebral Cortex (Peters A, Rockland KS, eds), pp 201-259. New York: Plenum Press.

Cellerino A, Maffei L, Domenici L (1996) The distribution of brain-derived neurotrophic factor and its receptor trkB in parvalbumin-containing neurons of the rat visual cortex. Eur J Neurosci 8:1190-1197.

Chow A, Erisir A, Farb C, Nadal MS, Ozaita A, Lau D, Welker E, Rudy B (1999) K(+) channel expression distinguishes subpopulations of parvalbumin- and somatostatin-containing neocortical interneurons. J Neurosci 19:9332-9345.

Clark AG, Glanowski S, Nielsen R, Thomas PD, Kejariwal A, Todd MA, Tanenbaum DM, Civello D, Lu F, Murphy B, Ferriera S, Wang G, Zheng X, White TJ, Sninsky JJ, Adams MD, Cargill M (2003) Inferring nonneutral evolution from human-chimp-mouse orthologous gene trios. Science 302:1960-1963.

Conde F, Lund JS, Jacobowitz DM, Baimbridge KG, Lewis DA (1994) Local circuit neurons immunoreactive for calretinin, calbindin D-28k or parvalbumin in monkey prefrontal cortex: distribution and morphology. J Comp Neurol 341:95-116.

Davis S, Bozon B, Laroche S (2003) How necessary is the activation of the immediate early gene zif268

in synaptic plasticity and learning? Behav Brain Res 142:17-30.

DeFelipe J (1993) Neocortical neuronal diversity: chemical heterogeneity revealed by colocalization studies of classic neurotransmitters, neuropeptides, calcium-binding proteins, and cell surface molecules. Cereb Cortex 3:273-289.

DeFelipe J (1997) Types of neurons, synaptic connections and chemical characteristics of cells immunoreactive for calbindin-D28K, parvalbumin and calretinin in the neocortex. J Chem Neuroanat 14:1-19.

DeFelipe J, Farinas I (1992) The pyramidal neuron of the cerebral cortex: morphological and chemical characteristics of the synaptic inputs. Prog Neurobiol 39:563-607.

DeFelipe J, Gonzalez-Albo MC, Del Rio MR, Elston GN (1999) Distribution and patterns of connectivity of interneurons containing calbindin, calretinin, and parvalbumin in visual areas of the occipital and temporal lobes of the macaque monkey. J Comp Neurol 412:515-526.

Ding Y, Casagrande VA (1998) Synaptic and neurochemical characterization of parallel pathways to the cytochrome oxidase blobs of primate visual cortex. J Comp Neurol 391:429-443.

Donoghue MJ, Rakic P (1999a) Molecular gradients and compartments in the embryonic primate cerebral cortex. Cereb Cortex 9:586-600.

Donoghue MJ, Rakic P (1999b) Molecular evidence for the early specification of presumptive functional domains in the embryonic primate cerebral cortex. J Neurosci 19:5967-5979.

Dorus S, Vallender EJ, Evans PD, Anderson JR, Gilbert SL, Mahowald M, Wyckoff GJ, Malcom CM, Lahn BT (2004) Accelerated Evolution of Nervous System Genes in the Origin of Homo sapiens. Cell 119:1027-1040.

Ducray A, Bondier JR, Michel G, Bon K, Millot JL, Propper A, Kastner A (2002) Recovery following peripheral destruction of olfactory neurons in young and adult mice. Eur J Neurosci 15:1907-1917.

Dufour A, Seibt J, Passante L, Depaepe V, Ciossek T, Frisen J, Kullander K, Flanagan JG, Polleux F, Vanderhaeghen P (2003) Area specificity and topography of thalamocortical projections are controlled by ephrin/Eph genes. Neuron 39:453-465.

Dzwonek J, Rylski M, Kaczmarek L (2004) Matrix metalloproteinases and their endogenous inhibitors in neuronal physiology of the adult brain. FEBS Lett 567:129-135.

Engel J, Taylor W, Paulsson M, Sage H, Hogan B (1987) Calcium binding domains and calcium-induced conformational transition of SPARC/BM-40/osteonectin, an extracellular glycoprotein expressed in mineralized and nonmineralized tissues. Biochemistry 26:6958-6965.

Fawcett JW, Asher RA (1999) The glial scar and central nervous system repair. Brain Res Bull 49:377-391.

Fitch MT, Silver J (1997) Glial cell extracellular matrix: boundaries for axon growth in development and regeneration. Cell Tissue Res 290:379-384.

Fitzpatrick D, Lund JS, Schmechel DE, Towles AC (1987) Distribution of GABAergic neurons and axon terminals in the macaque striate cortex. J Comp Neurol 264:73-91.

Fremeau RT, Jr., Troyer MD, Pahner I, Nygaard GO, Tran CH, Reimer RJ, Bellocchio EE, Fortin D, Storm-Mathisen J, Edwards RH (2001) The expression of vesicular glutamate transporters defines two classes of excitatory synapse. Neuron 31:247-260.

Glezer, II, Hof PR, Morgane PJ (1998) Comparative analysis of calcium-binding protein-immunoreactive neuronal populations in the auditory and visual systems of the bottlenose dolphin (Tursiops truncatus) and the macaque monkey (Macaca fascicularis). J Chem Neuroanat 15:203-237.

Glezer, II, Hof PR, Leranth C, Morgane PJ (1993) Calcium-binding protein-containing neuronal populations in mammalian visual cortex: a comparative study in whales, insectivores, bats, rodents, and primates. Cereb Cortex 3:249-272.

Hendrickson AE, Tillakaratne NJ, Mehra RD, Esclapez M, Erickson A, Vician L, Tobin AJ (1994) Differential localization of two glutamic acid decarboxylases (GAD65 and GAD67) in adult monkey visual cortex. J Comp Neurol 343:566-581.

Hof PR, Glezer, II, Nimchinsky EA, Erwin JM (2000) Neurochemical and cellular specializations in the mammalian neocortex reflect phylogenetic relationships: evidence from primates, cetaceans, and artiodactyls. Brain Behav Evol 55:300-310.

Hohenester E, Maurer P, Timpl R (1997) Crystal structure of a pair of follistatin-like and EF-hand calcium-binding domains in BM-40. Embo J 16:3778-3786.

Hubel DH, Wiesel TN (1972) Laminar and columnar distribution of geniculo-cortical fibers in the macaque monkey. J Comp Neurol 146:421-450.

Hubel DH, Wiesel TN (1998) Early exploration of the visual cortex. Neuron 20:401-412.

Ichinohe N, Rockland KS (2004) Region specific micromodularity in the uppermost layers in primate cerebral cortex. Cereb Cortex 14:1173-1184.

Illing RB (2001) Activity-dependent plasticity in the adult auditory brainstem. Audiol Neurootol 6:319-345.

Johnston IM, Spence HJ, Winnie JN, McGarry L, Vass JK, Meagher L, Stapleton G, Ozanne BW (2000) Regulation of a multigenic invasion programme by the transcription factor, AP-1: re-expression of a down-regulated gene, TSC-36, inhibits invasion. Oncogene 19:5348-5358.

Jones EG, Friedman DP (1982) Projection pattern of functional components of thalamic ventrobasal complex on monkey somatosensory cortex. J Neurophysiol 48:521-544.

Jones EG, Dell'Anna ME, Molinari M, Rausell E, Hashikawa T (1995) Subdivisions of macaque monkey auditory cortex revealed by calcium-binding protein immunoreactivity. J Comp Neurol 362:153-170.

Jones MW (2002) A comparative review of rodent prefrontal cortex and working memory. Curr Mol Med 2:639-647.

Kaas JH (1989) The evolution of complex sensory systems in mammals. J Exp Biol 146:165-176.

Katz LC, Shatz CJ (1996) Synaptic activity and the construction of cortical circuits. Science 274:1133-1138.

Kawaguchi Y, Kubota Y (1997) GABAergic cell subtypes and their synaptic connections in rat frontal cortex. Cereb Cortex 7:476-486.

Komatsu Y, Watakabe A, Hashikawa T, Tochitani S, Yamamori T (2005) Retinol-binding protein gene is highly expressed in higher-order association areas of the primate neocortex. Cereb Cortex 15:96-108.

Kondo H, Hashikawa T, Tanaka K, Jones EG (1994) Neurochemical gradient along the monkey occipito-temporal cortical pathway. Neuroreport 5:613-616.

Kondo H, Tanaka K, Hashikawa T, Jones EG (1999) Neurochemical gradients along monkey sensory cortical pathways: calbindin-immunoreactive pyramidal neurons in layers II and III. Eur J Neurosci 11:4197-4203.

Kondo M, Sumino R, Okado H (1997) Combinations of AMPA receptor subunit expression in individual cortical neurons correlate with expression of specific calcium-binding proteins. J Neurosci 17:1570-1581.

Krubitzer L (1995) The organization of neocortex in mammals: are species differences really so different? Trends Neurosci 18:408-417.

Land PW (1987) Dependence of cytochrome oxidase activity in the rat lateral geniculate nucleus on retinal innervation. J Comp Neurol 262:78-89.

Livingstone MS, Hubel DH (1982) Thalamic inputs to cytochrome oxidase-rich regions in monkey visual cortex. Proc Natl Acad Sci U S A 79:6098-6101.

Lund JS, Yoshioka T, Levitt JB (1994) Substrates for interlaminar connections in area V1 of macaque monkey cerebral cortex. In: Cerebral Cortex (Peters A, Rockland KS, eds), pp 37-60. New York: Plenum Press.

Lund JS, Henry GH, MacQueen CL, Harvey AR (1979) Anatomical organization of the primary visual cortex (area 17) of the cat. A comparison with area 17 of the macaque monkey. J Comp Neurol 184:599-618.

Markram H, Toledo-Rodriguez M, Wang Y, Gupta A, Silberberg G, Wu C (2004) Interneurons of the neocortical inhibitory system. Nat Rev Neurosci 5:793-807.

Marr HS, Edgell CJ (2003) Testican-1 inhibits attachment of Neuro-2a cells. Matrix Biol 22:259-266.

McCormick DA, Connors BW, Lighthall JW, Prince DA (1985) Comparative electrophysiology of pyramidal and sparsely spiny stellate neurons of the neocortex. J Neurophysiol 54:782-806.

Mendis DB, Brown IR (1994) Expression of the gene encoding the extracellular matrix glycoprotein SPARC in the developing and adult mouse brain. Brain Res Mol Brain Res 24:11-19.

Mendis DB, Shahin S, Gurd JW, Brown IR (1994) Developmental expression in the rat cerebellum of

SC1, a putative brain extracellular matrix glycoprotein related to SPARC. Brain Res 633:197-205.

Murphy WJ, Eizirik E, O'Brien SJ, Madsen O, Scally M, Douady CJ, Teeling E, Ryder OA, Stanhope MJ, de Jong WW, Springer MS (2001) Resolution of the early placental mammal radiation using Bayesian phylogenetics. Science 294:2348-2351.

Nakamura T, Takio K, Eto Y, Shibai H, Titani K, Sugino H (1990) Activin-binding protein from rat ovary is follistatin. Science 247:836-838.

Nie F, Wong-Riley MT (1996) Mitochondrial- and nuclear-encoded subunits of cytochrome oxidase in neurons: differences in compartmental distribution, correlation with enzyme activity, and regulation by neuronal activity. J Comp Neurol 373:139-155.

Nieuwenhuys R (1994) The neocortex. An overview of its evolutionary development, structural organization and synaptology. Anat Embryol (Berl) 190:307-337.

O'Leary DD (1989) Do cortical areas emerge from a protocortex? Trends Neurosci 12:400-406.

O'Leary DD, Nakagawa Y (2002) Patterning centers, regulatory genes and extrinsic mechanisms controlling arealization of the neocortex. Curr Opin Neurobiol 12:14-25.

Parvizi J, Damasio AR (2003) Differential distribution of calbindin D28k and parvalbumin among functionally distinctive sets of structures in the macaque brainstem. J Comp Neurol 462:153-167.

Patel K, Connolly DJ, Amthor H, Nose K, Cooke J (1996) Cloning and early dorsal axial expression of Flik, a chick follistatin- related gene: evidence for involvement in dorsalization/neural induction. Dev Biol 178:327-342.

Pavlov I, Lauri S, Taira T, Rauvala H (2004) The role of ECM molecules in activity-dependent synaptic development and plasticity. Birth Defects Res Part C Embryo Today 72:12-24.

Paxinos G, Franklin K (2001) The mouse brain in stereotaxic coordinates, 2nd Edition. San Diego USA: Acadedemic Press.

Paxinos G, Huang X, Toga A (2000) The rhesus monkey brain in stereotaxic coodinates. San Diego, USA: Academic Press.

Pizzorusso T, Medini P, Berardi N, Chierzi S, Fawcett JW, Maffei L (2002) Reactivation of ocular dominance plasticity in the adult visual cortex. Science 298:1248-1251.

Preuss TM, Kaas JH (1996) Parvalbumin-like immunoreactivity of layer V pyramidal cells in the motor and somatosensory cortex of adult primates. Brain Res 712:353-357.

Preuss TM, Caceres M, Oldham MC, Geschwind DH (2004) Human brain evolution: insights from microarrays. Nat Rev Genet 5:850-860.

Rakic P (1988) Specification of cerebral cortical areas. Science 241:170-176.

Revishchin AV, Garey LJ (1991) Laminar distribution of cytochrome oxidase staining in cetacean isocortex. Brain Behav Evol 37:355-367.

Rockel AJ, Hiorns RW, Powell TP (1980) The basic uniformity in structure of the neocortex. Brain 103:221-244.

Rubenstein JL, Anderson S, Shi L, Miyashita-Lin E, Bulfone A, Hevner R (1999) Genetic control of cortical regionalization and connectivity. Cereb Cortex 9:524-532.

Schlaggar BL, O'Leary DD (1991) Potential of visual cortex to develop an array of functional units unique to somatosensory cortex. Science 252:1556-1560.

Schnepp A, Komp Lindgren P, Hulsmann H, Kroger S, Paulsson M, Hartmann U (2005) Mouse testican-2. Expression, glycosylation, and effects on neurite outgrowth. J Biol Chem 280:11274-11280.

Seibt J, Schuurmans C, Gradwhol G, Dehay C, Vanderhaeghen P, Guillemot F, Polleux F (2003) Neurogenin2 specifies the connectivity of thalamic neurons by controlling axon responsiveness to intermediate target cues. Neuron 39:439-452.

Sekirnjak C, Martone ME, Weiser M, Deerinck T, Bueno E, Rudy B, Ellisman M (1997) Subcellular localization of the K+ channel subunit Kv3.1b in selected rat CNS neurons. Brain Res 766:173-187.

Serfilippi LM, Pallman DR, Gruebbel MM, Kern TJ, Spainhour CB (2004) Assessment of retinal degeneration in outbred albino mice. Comp Med 54:69-76.

Shibanuma M, Mashimo J, Mita A, Kuroki T, Nose K (1993) Cloning from a mouse osteoblastic cell line of a set of transforming- growth-factor-beta 1-regulated genes, one of which seems to encode a follistatin-related polypeptide. Eur J Biochem 217:13-19.

Spatz WB, Illing RB, Weisenhorn DM (1994) Distribution of cytochrome oxidase and parvalbumin in the primary visual cortex of the adult and neonate monkey, Callithrix jacchus. J Comp Neurol 339:519-534.

Takahata T, Komatsu Y, Watakabe A, Yamamori T (2004) Comparative analysis of transcription patterns of *occ1/frp* in mammalian brains. In: Society for Neuroscience. San Diego.

Takamori S, Rhee JS, Rosenmund C, Jahn R (2000) Identification of a vesicular glutamate transporter that defines a glutamatergic phenotype in neurons. Nature 407:189-194.

Tanaka M, Ozaki S, Osakada F, Mori K, Okubo M, Nakao K (1998) Cloning of follistatin-related protein as a novel autoantigen in systemic rheumatic diseases. Int Immunol 10:1305-1314.

Tanaka M, Ozaki S, Kawabata D, Kishimura M, Osakada F, Okubo M, Murakami M, Nakao K, Mimori T (2003) Potential preventive effects of follistatin-related protein/TSC-36 on joint destruction and antagonistic modulation of its autoantibodies in rheumatoid arthritis. Int Immunol 15:71-77.

Tochitani S, Hashikawa T, Yamamori T (2003) Expression of occ1 mRNA in the visual cortex during postnatal development in macaques. Neurosci Lett 337:114-116.

Tochitani S, Liang F, Watakabe A, Hashikawa T, Yamamori T (2001) The occ1 gene is preferentially expressed in the primary visual cortex in an activity-dependent manner: a pattern of gene expression related to the cytoarchitectonic area in adult macaque neocortex. Eur J Neurosci

13:297-307.

Toledo-Rodriguez M, Blumenfeld B, Wu C, Luo J, Attali B, Goodman P, Markram H (2004) Correlation maps allow neuronal electrical properties to be predicted from single-cell gene expression profiles in rat neocortex. Cereb Cortex 14:1310-1327.

Tremble PM, Lane TF, Sage EH, Werb Z (1993) SPARC, a secreted protein associated with morphogenesis and tissue remodeling, induces expression of metalloproteinases in fibroblasts through a novel extracellular matrix-dependent pathway. J Cell Biol 121:1433-1444.

Tsuchida K, Arai KY, Kuramoto Y, Yamakawa N, Hasegawa Y, Sugino H (2000) Identification and characterization of a novel follistatin-like protein as a binding protein for the TGF-beta family. J Biol Chem 275:40788-40796.

Van Brederode JF, Mulligan KA, Hendrickson AE (1990) Calcium-binding proteins as markers for subpopulations of GABAergic neurons in monkey striate cortex. J Comp Neurol 298:1-22.

Vannahme C, Gosling S, Paulsson M, Maurer P, Hartmann U (2003) Characterization of SMOC-2, a modular extracellular calcium-binding protein. Biochem J 373:805-814.

Vannahme C, Schubel S, Herud M, Gosling S, Hulsmann H, Paulsson M, Hartmann U, Maurer P (1999) Molecular cloning of testican-2: defining a novel calcium-binding proteoglycan family expressed in brain. J Neurochem 73:12-20.

Verhaagen J, Oestreicher AB, Grillo M, Khew-Goodall YS, Gispen WH, Margolis FL (1990) Neuroplasticity in the olfactory system: differential effects of central and peripheral lesions of the primary olfactory pathway on the expression of B-50/GAP43 and the olfactory marker protein. J Neurosci Res 26:31-44.

Vertegaal AC, Kuiperij HB, van Laar T, Scharnhorst V, van der Eb AJ, Zantema A (2000) cDNA micro array identification of a gene differentially expressed in adenovirus type 5- versus type 12-transformed cells. FEBS Lett 487:151-155.

Wang Y, Gupta A, Toledo-Rodriguez M, Wu CZ, Markram H (2002) Anatomical, physiological, molecular and circuit properties of nest basket cells in the developing somatosensory cortex. Cereb Cortex 12:395-410.

Watakabe A, Fujita H, Hayashi M, Yamamori T (2001a) Growth/differentiation factor 7 is preferentially expressed in the primary motor area of the monkey neocortex. J Neurochem 76:1455-1464.

Watakabe A, Sugai T, Nakaya N, Wakabayashi K, Takahashi H, Yamamori T, Nawa H (2001b) Similarity and variation in gene expression among human cerebral cortical subregions revealed by DNA macroarrays: technical consideration of RNA expression profiling from postmortem samples. Brain Res Mol Brain Res 88:74-82.

White LE, Coppola DM, Fitzpatrick D (2001) The contribution of sensory experience to the maturation of orientation selectivity in ferret visual cortex. Nature 411:1049-1052.

Williams SM, Goldman-Rakic PS, Leranth C (1992) The synaptology of parvalbumin-immunoreactive

neurons in the primate prefrontal cortex. J Comp Neurol 320:353-369.

Wong-Riley M (1979) Changes in the visual system of monocularly sutured or enucleated cats demonstrable with cytochrome oxidase histochemistry. Brain Res 171:11-28.

Wong-Riley MT, Welt C (1980) Histochemical changes in cytochrome oxidase of cortical barrels after vibrissal removal in neonatal and adult mice. Proc Natl Acad Sci U S A 77:2333-2337.

Woolsey TA, Welker C, Schwartz RH (1975) Comparative anatomical studies of the SmL face cortex with special reference to the occurrence of "barrels" in layer IV. J Comp Neurol 164:79-94.

Yan Q, Sage EH (1999) SPARC, a matricellular glycoprotein with important biological functions. J Histochem Cytochem 47:1495-1506.

Zaitsev AV, Gonzalez-Burgos G, Povysheva NV, Kroner S, Lewis DA, Krimer LS (2005) Localization of Calcium-binding Proteins in Physiologically and Morphologically Characterized Interneurons of Monkey Dorsolateral Prefrontal Cortex. Cereb Cortex 15:1178-1186

Zaremba S, Guimaraes A, Kalb RG, Hockfield S (1989) Characterization of an activity-dependent, neuronal surface proteoglycan identified with monoclonal antibody Cat-301. Neuron 2:1207-1219.

Zwijsen A, Blockx H, Van Arnhem W, Willems J, Fransen L, Devos K, Raymackers J, Van de Voorde A, Slegers H (1994) Characterization of a rat C6 glioma-secreted follistatin-related protein (FRP). Cloning and sequence of the human homologue. Eur J Biochem 225:937-946.

Abbreviations

A1/ primary auditory cortex; AP/ alkaline phosphatase; BM-40/ basement membrane-40; CO/ cytochrome oxidase; CB/ calbindin D28-K; CR/ calretinin; CSPG/ chondroitin sulphate proteoglycan; DAB/ 3'3-diaminobenzidine; dLGN/ dorsal lateral geniculate nucleus; DIG/ digoxigenin; DNP/ dinitrophenyl; EC domain/ extracellular Ca^{2+}-binding domain; ECM/ extracellular matrix; EDTA/ ethylenediamine-N,N,N',N'-tetraacetic acid; FITC/ fluorescein; FRP/ follistatin-related protein; FS domain/ follistatin-like domain; GABA/ γ-amino butyric acid; GAD67/ glutamic acid decarboxylase 67; GAP43/ growth associated protein 43; HNPP/ 2-hydroxy-3-naphtoic acid-2'-phenylanilide phosphate; HRP/ horseradish peroxidase; ISH/ *in situ* hybridization; NIBB/ national institute for basic biology; NIH/ national institutes of health ; NLS/ N-lauroylsarcosine; OMP/ olfactory marker protein; PB/ phosphate buffer; PBS/ phosphate-buffered saline; PFA/ paraformaldehyde; PV/ parvalbumin; SDS/ sodium dodecylsulphate; SPARC/ secreted protein, acidic and rich in cystein; SSC/ saline sodium citrate; TE/ temporal cortex; TEO/ occipital temporal cortex; TGF-β/ transforming growth factor-β; TSC-36/ TGF-β1-stimulated clone 36; TTX/ tetrodotoxin; V1/ primary visual cortex; V2/ secondary visual cortex; VGLUT1/ vesicular glutamate transporter 1